

Vector and Tensor Microwave Background Signatures of a Primordial Stochastic Magnetic Field

Andrew Mack^{1†}, Tina Kahnishvili^{1,2‡}, and Arthur Kosowsky^{1†}

¹*Department of Physics and Astronomy, Rutgers University, 136 Frelinghuysen Road, Piscataway, New Jersey 08854-8019*

²*Center for Plasma Astrophysics, Abastumani Astrophysical Observatory, A. Kazbegi Ave. 2a, 380060 Tbilisi, Georgia*

† andymack, kosowsky@physics.rutgers.edu, ‡tinatin@amorgos.unige.ch

A stochastic magnetic field in the early Universe will produce anisotropies in the temperature and polarization of the cosmic microwave background. We derive analytic expressions for the microwave background temperature and polarization power spectra induced by vector and tensor perturbations from a power-law magnetic field. For a scale-invariant stochastic magnetic field with a comoving damping scale of 1.4 Mpc, current microwave background temperature measurements constrain the comoving mean-field amplitude to be no greater than approximately 6×10^{-10} G. Limits improve as the power-law slope increases: for causally-generated power-law magnetic fields, the comoving mean-field amplitude has an upper bound of approximately 3×10^{-11} G. These are the strongest current limits on large-scale primordial magnetic fields.

98.70.Vc, 98.62.En, 98.80.Cq, 98.80.Hw

I. INTRODUCTION

Magnetic fields of μ G strength are ubiquitous in galaxies [1] and clusters of galaxies [2]. The origin of these fields, however, remains an outstanding problem in cosmology. It is usually postulated that these μ G fields grew either via some magnetohydrodynamical (MHD) dynamo mechanism [3,4] or via adiabatic compression of a primordial magnetic field during the collapse of a protogalactic cloud. A MHD dynamo requires tiny seed magnetic fields of comoving amplitude 10^{-20} G in conventional CDM-like cosmological models or even as tiny as 10^{-30} G in a Universe with a non-zero cosmological constant [5] as suggested by recent measurements of type Ia supernovae [6,7] and the microwave background power spectrum [8–12]. On the other hand, the adiabatic compression scenario requires a far larger primordial seed field with comoving amplitude of 10^{-9} G to 10^{-10} G.

Persistent questions about the effectiveness of MHD dynamos [13–20] together with the observation of μ G magnetic fields in high-redshift galaxies [1] raise the possibility of a significant primordial magnetic field in galaxies and clusters of galaxies. The origin of such a magnetic field remains a mystery. Essentially all viable magnetogenesis mechanisms incorporate speculative ideas in high-energy theory, including (among others) inflation [21–26], electroweak [27,28] or QCD [29,30] phase transitions, charge asymmetry [31], or a ferromagnetic Yang–Mills vacuum state [32]. As the properties of the primordial magnetic field predicted varies among these mechanisms, future detections of a primordial magnetic field may aid us in identifying the correct magnetogenesis mechanism. On the cosmological front, a primordial magnetic field may have affected early-Universe processes such as phase transitions, baryogenesis, and nucleosynthesis (see [33] for a review). Relic magnetic fields could provide a unique direct source of information about these processes. A primordial magnetic field may also have influenced structure formation via contributing to density perturbations on galactic scales [34,35] and preserving magnetic energy in Alfvén modes on scales below the Silk damping scale during recombination [36,37]. In short, significant primordial magnetic fields would impact both cosmology and particle physics.

The presence of a magnetic field in the early Universe affects the evolution of metric perturbations, and as a result, produces temperature and polarization anisotropies in the cosmic microwave background (CMB). High-resolution measurements of the microwave background provide a clean and model-independent test for primordial magnetic fields. We demonstrate in this paper that fields large enough to result in observed fields via adiabatic compression will likely leave observable and distinctive fluctuations in the various power spectra of microwave background temperature and polarization fluctuations.

Substantial progress has been made in understanding the effects of a primordial magnetic field on the CMB. The case of a homogeneous magnetic field has been considered by several authors. The best current constraint on the primordial homogeneous magnetic field strength is $B_0 < 3.4 \times 10^{-9} (\Omega_0 h_{50}^2)^{1/2}$ G (h_{50} is the present Hubble constant in units of $50 \text{ km s}^{-1} \text{ Mpc}^{-1}$), obtained by doing statistical analysis on the 4-year Cosmic Background Explorer (COBE) data for temperature patterns of a Bianchi type VII anisotropic spacetime [38]. A primordial homogeneous magnetic field can produce distortions of the CMB acoustic peaks via fast magnetosonic waves [39]; meanwhile, Alfvén wave excitations can amplify vector perturbations and induce additional correlations in temperature multipole moments

[40]. It is shown in Ref. [41] that a primordial homogeneous magnetic field of present strength 10^{-9} G at decoupling can induce a measurable Faraday rotation in the CMB polarization of 1° at a frequency of 30 GHz. Additional CMB polarization effects arising from a primordial homogeneous magnetic field via Faraday rotation include a parity-odd cross-correlation between temperature and polarization anisotropies [42] and the depolarization of the original CMB polarization [43], which leads to a reduction in the damping of temperature anisotropies on small angular scales.

The case of a stochastic magnetic field is perhaps more realistic, because such fields are observed within galaxy clusters [44–47] and predicted by all causal magnetogenesis mechanisms [33]. Some numerical estimates of CMB temperature and polarization power spectra from density perturbations induced by a primordial stochastic magnetic field are presented in Ref. [48], whereas corresponding analytic estimates, though somewhat crude and valid only for temperature anisotropies on large angular scales, are given in Ref. [49]. Effects of Alfvén waves induced by a primordial stochastic magnetic field on CMB temperature and B-type polarization anisotropies are considered in Refs. [50] and [51] respectively, with analytic estimates of the power spectra given for a single Fourier mode. Finally, a primordial stochastic magnetic field also generates gravitational waves; the resulting tensor CMB temperature power spectrum is given in Ref. [52].

Although a variety of effects of a primordial stochastic magnetic field on the CMB have been investigated, the results are fragmented and a systematic approach is lacking. Besides the temperature power spectrum from tensor perturbations given in Ref. [52], no other CMB power spectra have been derived. We consider a statistically homogeneous and isotropic stochastic magnetic field with a power-law power spectrum, generated at some early epoch of the radiation-dominated Universe. Based on the computational techniques in Ref. [52] and the total angular momentum method for calculating CMB anisotropies introduced by Hu and White [53], we have completed a comprehensive and unified analytic calculation of all types of CMB power spectra arising from a primordial stochastic magnetic field. This paper focusses on the induced vector and tensor perturbations. A primordial magnetic field acts as a continuous source of vorticity until decoupling and gravitational radiation until matter-radiation equality. The resulting vector and tensor perturbations are one of the few cosmological sources of B-type polarization [54,55], along with primordial tensor perturbations [56] and gravitational lensing of the CMB [57]. A companion paper [58] discusses the corresponding scalar perturbations.

In Sec. II we derive the power spectrum for a primordial stochastic magnetic field. We then project the vector and tensor pieces from the electromagnetic stress-energy tensor, from which we calculate their two-point correlation functions and derive their isotropic spectra. Details of the derivation of the vector isotropic spectrum are presented in the Appendix. In Sec. III we review the vector and tensor contributions to the metric tensor and give their corresponding evolution equations. We obtain solutions to these equations, which can be expressed as functions of the magnetic-induced isotropic spectra derived in Sec. II. Using the total angular momentum method of Ref. [53], we compute analytically the CMB power spectra for temperature in Sec. IV, polarization in Sec. V, and the temperature-polarization cross correlation in Sec. VI. Section VII concludes with the physical interpretation of these results and a discussion of current and future limits on primordial magnetic fields from the microwave background. For the vector perturbations, the polarization and cross-correlation power spectra are all essentially identical; whereas for the tensor perturbations, the polarization power spectra are comparable to the temperature power spectrum for $n > 0$, where n is the magnetic field power-law index. For a scale-invariant $n \rightarrow -3$ stochastic magnetic field with a comoving damping scale of 1.4 Mpc, current microwave background temperature measurements constrain the comoving mean-field amplitude to be no greater than approximately 6×10^{-10} G. Limits improve as n increases: for causally-generated power-law magnetic fields with $n \geq 2$, the comoving mean-field amplitude has an upper bound of approximately 3×10^{-11} G. These are the strongest current limits on large-scale primordial magnetic fields.

For simplicity, we consider the case of a flat Universe. We employ notational conventions similar to those in Ref. [53]; a is the scale factor, η is the conformal time, overdots are derivatives with respect to η , and 0 subscripts denote the present time. We set $c = 1$ and normalize the scale factor to unity today. As usual, Greek indices run from 0 to 3 and Latin ones from 1 to 3. All calculations are done in Fourier space. Where confusion may arise, such as when discussing the normalization of the magnetic correlation function in Sec. II and the Lorentz force vector in Sec. II A, we restore the real-space dependence. All magnetic field amplitudes are comoving values, unless an explicit time dependence is displayed.

II. MAGNETIC POWER SPECTRUM AND CORRELATION FUNCTIONS

Consider a primordial stochastic magnetic field created at some specific moment during the radiation-dominated epoch. The energy density of the magnetic field is treated as a first-order perturbation to a flat Friedmann-Robertson-Walker (FRW) background cosmology. Within the linear approximation, the magnetic field evolves as a stiff source and we discard all MHD fluid back reactions onto the field itself [52]. Prior to decoupling, the conductivity of the

primordial plasma is very large [21,59] and for practical purposes can be assumed infinite. In the comoving frame, this implies the “frozen-in” condition $\mathbf{E} = -\mathbf{v} \times \mathbf{B}$, where \mathbf{v} is the plasma peculiar velocity and \mathbf{E} is the electric field induced by plasma motions. Infinite conductivity leads to a vanishing electric field in linear perturbation theory ($v \ll 1$) and allows the time evolution of the magnetic field to decouple from its spatial structure on sufficiently large scales. As the Universe expands, magnetic field lines are simply conformally diluted due to flux conservation: $\mathbf{B}(\eta, \mathbf{x}) = \mathbf{B}(\mathbf{x})/a^2$. On small scales, however, a primordial magnetic field is damped due to photon and neutrino viscosities [36,37]. As in Ref. [52], we parametrize this damping by introducing a hard ultraviolet cutoff k_D in the magnetic power spectrum. The choice for this cutoff value will be discussed in Sec. VII.

A statistically homogeneous and isotropic magnetic field must have the two-point correlation function [52,60]

$$\langle B_i(\mathbf{k}) B_j^*(\mathbf{k}') \rangle = (2\pi)^3 P_{ij} P(k) \delta(\mathbf{k} - \mathbf{k}'), \quad (2.1)$$

where

$$P_{ij} \equiv \delta_{ij} - \hat{k}_i \hat{k}_j \quad (2.2)$$

is a projector onto the transverse plane:

$$P_{ij} P_{jk} = P_{ik}, \quad P_{ij} \hat{k}_j = 0, \quad (2.3)$$

and $\hat{k}_i = k_i/k$. We adopt the Fourier transform convention

$$B_i(\mathbf{k}) = \int d^3x \exp(i\mathbf{k} \cdot \mathbf{x}) B_i(\mathbf{x}). \quad (2.4)$$

Note the projection tensor of Eq. (2.2) is valid only for the case of a flat Universe where perturbations can be decomposed into plane waves; for non-zero spatial curvatures, the analog to a plane-wave basis must be employed (see, e.g., [61]). A specific magnetogenesis model consists of specifying the function $P(k)$, which we take to be a power law

$$P(k) = A k^n. \quad (2.5)$$

Our primary interest is to constrain the present magnetic field strength. We smooth the field over the comoving magnetic-damping scale λ_D , $B_i(\mathbf{k}) \rightarrow B_i(\mathbf{k}) * f_k^D$, where $f_k^D = \exp(-\lambda_D^2 k^2/2)$ is the 3D-Gaussian filter transform of radius λ_D , and normalize as

$$\langle B_i(\mathbf{x}) B_i(\mathbf{x}) \rangle |_{\lambda_D} = B_0^2. \quad (2.6)$$

Thus B_0 is the rms magnetic field strength today smoothed over λ_D . This mean-square value is then given by the Fourier transform of the product of the power spectrum $P(k)$ and the square of the filter transform f_k^D ,

$$B_0^2 = \frac{1}{(2\pi)^3} \int d^3k P(k) |f_k^D|^2 \simeq \frac{A}{(2\pi)^2} \frac{1}{\lambda_D^{n+3}} \Gamma\left(\frac{n+3}{2}\right). \quad (2.7)$$

We require the spectral index $n > -3$ to prevent infrared divergence of the integral over the spectrum of long wavelengths $k \rightarrow 0$. Solving for the normalization A and using Eqs. (2.1) and (2.5), we arrive at the two-point correlation function for a primordial stochastic magnetic field

$$\langle B_i(\mathbf{k}) B_j^*(\mathbf{k}') \rangle = (2\pi)^{n+8} \frac{B_0^2}{\Gamma\left(\frac{n+3}{2}\right)} P_{ij} \frac{k^n}{k_D^{n+3}} \delta(\mathbf{k} - \mathbf{k}'), \quad k < k_D, \quad (2.8)$$

where $k_D = 2\pi/\lambda_D$. The spectrum vanishes for all scales smaller than the damping scale $k > k_D$. The condition $n > -3$ guarantees that superhorizon coherent fields are not overproduced; the limit $n \rightarrow -3$ approaches a scale-invariant spectrum. The case $n = 0$ corresponds to a white noise spectrum where we have equal power at all wavelengths. For a causally-generated stochastic magnetic field, we require $n \geq 2$ [52,60,62].

The induced electromagnetic stress-energy tensor is given by the convolution of the magnetic field [63]

$$\tau_{ij}^{(B)}(\mathbf{k}) = \frac{1}{(2\pi)^3} \frac{1}{4\pi} \int d^3p \left[B_i(\mathbf{p}) B_j(\mathbf{k} - \mathbf{p}) - \frac{1}{2} \delta_{ij} B_l(\mathbf{p}) B_l(\mathbf{k} - \mathbf{p}) \right]. \quad (2.9)$$

It can be geometrically decomposed into scalar, vector, and tensor perturbation modes, $\tau_{ij}^{(B)} = \Pi_{ij}^{(S)} + \Pi_{ij}^{(V)} + \Pi_{ij}^{(T)}$, according to their three-space coordinate transformation properties on the constant-time hypersurface [64]. In the linear approximation, all types of cosmological perturbations are decoupled from each other dynamically; thus we can consider each type of perturbation independently. From the tensor $\Pi_{ij}^{(V)}$ we can construct a vector $\Pi_i^{(V)}$ that sources the vorticity perturbations, whereas the tensor $\Pi_{ij}^{(T)}$ sources the gravitational wave perturbations. To obtain CMB power spectra, we need to derive two-point correlation functions for $\Pi_i^{(V)}$ and $\Pi_{ij}^{(T)}$ and extract their corresponding isotropic spectra $|\Pi^{(V),(T)}(k)|^2$ as a function of B_0 , n , and k_D . This is the subject to which we now turn.

A. Vector Projection and Correlation Function

We begin by illustrating how to project from a generic spatial metric perturbation δg_{ij} its vector piece $\delta g_{ij}^{(V)}$. A vector spatial metric perturbation must have the form [64]

$$\delta g_{ij}^{(V)} = \xi_i \hat{k}_j + \xi_j \hat{k}_i, \quad (2.10)$$

where ξ_i is a divergenceless three vector. A possible construction for ξ_i is given by

$$\xi_i = \hat{k}_m \delta g_{mi} - \hat{k}_i \hat{k}_m \hat{k}_n \delta g_{mn}. \quad (2.11)$$

The projection then follows from substituting Eq. (2.11) into Eq. (2.10):

$$\delta g_{ij}^{(V)} = (\hat{k}_m \delta g_{mi} - \hat{k}_i \hat{k}_m \hat{k}_n \delta g_{mn}) \hat{k}_j + (\hat{k}_m \delta g_{mj} - \hat{k}_j \hat{k}_m \hat{k}_n \delta g_{mn}) \hat{k}_i = (P_{in} \hat{k}_j + P_{jn} \hat{k}_i) \hat{k}_m \delta g_{mn}. \quad (2.12)$$

Using Eq. (2.12), the vector part of the electromagnetic stress-energy tensor is given by

$$\Pi_{ij}^{(V)} = (P_{in} \hat{k}_j + P_{jn} \hat{k}_i) \hat{k}_m \tau_{mn}^{(B)}, \quad (2.13)$$

from which we can construct a vector $\Pi_i^{(V)}$ via contracting with the unit vector \hat{k}_j ,

$$\Pi_i^{(V)} = \Pi_{ij}^{(V)} \hat{k}_j = P_{in} \hat{k}_m \tau_{mn}^{(B)}. \quad (2.14)$$

The physical meaning of $\Pi_i^{(V)}$ is clear upon examining the Lorentz force vector. In the infinite conductivity limit, the Lorentz force vector in real space is given by [49,63]

$$\mathbf{L}(\mathbf{x}) \simeq -\frac{1}{4\pi} \{ \mathbf{B}(\mathbf{x}) \times [\nabla \times \mathbf{B}(\mathbf{x})] \} = \frac{1}{4\pi} \left\{ [\mathbf{B}(\mathbf{x}) \cdot \nabla] \mathbf{B}(\mathbf{x}) - \frac{1}{2} \nabla B^2(x) \right\}. \quad (2.15)$$

Fourier transforming Eq. (2.15), extracting the corresponding vortical component $L_i^{(V)}$ which satisfies the divergenceless condition $L_i^{(V)} \hat{k}_i = 0$, and comparing with Eq. (2.14) shows that

$$L_i^{(V)} = k \Pi_i^{(V)}. \quad (2.16)$$

The vector $\Pi_i^{(V)}$ will appear in the evolution equations for vector perturbations in Sec. III A.

The stochastic and transverse nature of $\Pi_i^{(V)}$ lead us to define the two-point correlation function

$$\langle \Pi_i^{(V)}(\mathbf{k}) \Pi_j^{(V)*}(\mathbf{k}') \rangle \equiv P_{ij} |\Pi^{(V)}(k)|^2 \delta(\mathbf{k} - \mathbf{k}'). \quad (2.17)$$

The vector isotropic spectrum $|\Pi^{(V)}(k)|^2$ can be obtained using Eq. (2.14) for $\Pi_i^{(V)}$, evaluating the two-point correlation function of the electromagnetic stress-energy tensor of Eq. (2.9), and comparing the result with Eq. (2.17). A lengthy calculation in the Appendix gives

$$|\Pi^{(V)}(k)|^2 \simeq \frac{(2\pi)^{2n+9}}{4} \frac{B_0^4}{\Gamma^2(\frac{n+3}{2})(2n+3)k_D^3} \left[1 + \frac{n}{n+3} \left(\frac{k}{k_D} \right)^{2n+3} \right], \quad k < k_D. \quad (2.18)$$

The first term dominates when $n > -3/2$, whereas the second term dominates when $-3 < n < -3/2$. For the case $n > -3/2$, the vector isotropic spectrum depends on the ultraviolet cutoff k_D , since the source contribution peaks at small scales. Note that the second term does *not* depend on k_D : B_0^4/k_D^{2n+6} is a constant proportional to the square of the magnetic power spectrum normalization [see Eq. (2.7)]. To simplify the calculation, we will only consider the corresponding dominant term for a given spectral index n , although including the contributions from both terms is a straightforward extension of the calculation presented here. In the neighborhood of $n = -3/2$, both terms must be included to handle correctly the removable singularity.

B. Tensor Projection and Correlation Function

Gravitational radiation is produced by the transverse and traceless piece of the electromagnetic stress-energy tensor, given by (see, e.g., [52])

$$\Pi_{ij}^{(T)} = (P_{im}P_{jn} - \frac{1}{2}P_{ij}P_{mn})\tau_{mn}^{(B)}. \quad (2.19)$$

It follows from the transverse and traceless properties of the tensor $\Pi_{ij}^{(T)}$ that its two-point correlation function can be written as [52]

$$\langle \Pi_{ij}^{(T)}(\mathbf{k}) \Pi_{lm}^{(T)*}(\mathbf{k}') \rangle \equiv \mathcal{M}_{ijlm} |\Pi^{(T)}(k)|^2 \delta(\mathbf{k} - \mathbf{k}'). \quad (2.20)$$

The tensor structure \mathcal{M}_{ijlm} is

$$\begin{aligned} \mathcal{M}_{ijlm} &\equiv P_{il}P_{jm} + P_{im}P_{jl} - P_{ij}P_{lm} \\ &= \delta_{il}\delta_{jm} + \delta_{im}\delta_{jl} - \delta_{ij}\delta_{lm} + \hat{k}_i\hat{k}_j\hat{k}_l\hat{k}_m \\ &\quad + \delta_{ij}\hat{k}_l\hat{k}_m + \delta_{lm}\hat{k}_i\hat{k}_j - \delta_{il}\hat{k}_j\hat{k}_m - \delta_{jm}\hat{k}_i\hat{k}_l - \delta_{im}\hat{k}_j\hat{k}_l - \delta_{jl}\hat{k}_i\hat{k}_m \end{aligned} \quad (2.21)$$

and satisfies $\mathcal{M}_{ijij} = 4$ and $\mathcal{M}_{iilm} = \mathcal{M}_{ijll} = 0$. The tensor isotropic spectrum $|\Pi^{(T)}(k)|^2$ can be obtained using Eq. (2.19) for $\Pi_{ij}^{(T)}$, evaluating the two-point correlation function of the electromagnetic stress-energy tensor of Eq. (2.9), and comparing the result with Eq. (2.20). A similar calculation as in the case of the vector isotropic spectrum gives

$$|\Pi^{(T)}(k)|^2 \simeq \frac{(2\pi)^{2n+9}}{8} \frac{B_0^4}{\Gamma^2(\frac{n+3}{2})(2n+3)k_D^3} \left[1 + \frac{n}{n+3} \left(\frac{k}{k_D} \right)^{2n+3} \right], \quad k < k_D. \quad (2.22)$$

The tensor isotropic spectrum differs from its vector counterpart only by a factor of two, due to the ratio of traces of their corresponding tensor structures P_{ij} and \mathcal{M}_{ijlm} . Again, the first term dominates when $n > -3/2$, whereas the second term dominates when $-3 < n < -3/2$. For the case $n > -3/2$, the tensor isotropic spectrum depends on the ultraviolet cutoff k_D ; the resulting tensor CMB temperature power spectrum then possesses the well-known behavior of a white noise source, $l^2 C_l \propto l^3$ [52]. We will demonstrate that this is also true for tensor CMB polarization and temperature-polarization cross-correlation. As with the vector case, we will only consider the dominant term of Eq. (2.22) for a given spectral index n .

III. METRIC PERTURBATIONS AND THEIR EVOLUTION

A primordial stochastic magnetic field generates CMB anisotropies via its gravitational effects on the metric tensor. The full metric tensor can be decomposed into its background and perturbation pieces, $g_{\mu\nu} = g_{\mu\nu}^{(0)} + \delta g_{\mu\nu}$; for a flat Universe with the usual conformal FRW metric, $g_{\mu\nu}^{(0)} = a^2 \eta_{\mu\nu}$, where $\eta_{\mu\nu} = \text{diag}(-1, 1, 1, 1)$ is the Minkowski metric tensor. The vector (Sec. III A) and tensor (Sec. III B) perturbations are calculated separately; the scalar perturbations are somewhat more complicated and are covered in a companion paper [58]. We review the various metric tensor contributions and give the corresponding evolution equations due to a primordial stochastic magnetic field. We then obtain solutions to these equations, which can be expressed as functions of the isotropic spectra derived in Sec. II.

A. Vector Perturbations

Vector perturbations to the geometry are described by two divergenceless three-vectors ζ_i and ξ_i with the general form [see Eq. (2.10) also]

$$\delta g_{0i}^{(V)} = -a^2 \zeta_i, \quad \delta g_{ij}^{(V)} = a^2 (\xi_i \hat{k}_j + \xi_j \hat{k}_i). \quad (3.1)$$

Vector perturbations represent vorticity; the divergenceless condition for vectors ζ_i and ξ_i guarantees the absence of density perturbations. Vector perturbations exhibit gauge freedom, which arises because the mapping of coordinates

between the perturbed physical manifold and the background is not unique. From vectors ζ_i and ξ_i , we can construct a gauge-invariant vector potential $V_i = \zeta_i + \dot{\xi}_i/k$ that geometrically describes the vector perturbations of the extrinsic curvature [65,66]. We now exploit the gauge freedom by explicitly choosing ξ_i to be a constant vector in time; it follows that $\delta g_{0i}^{(V)} = -a^2 V_i$. Vector perturbations of the stress-energy tensor can be parametrized by a divergenceless three-vector $\mathbf{v}^{(V)}$ that perturbs the four-velocity $u_\mu = (1, 0, 0, 0)$ of a stationary fluid element in the comoving frame [40]:

$$\delta u_\mu = (0, \mathbf{v}^{(V)}/a). \quad (3.2)$$

We can now construct a gauge-invariant, divergenceless three-vector termed the “vorticity,”

$$\Omega_i = v_i^{(V)} - V_i. \quad (3.3)$$

Two Einstein equations govern vector perturbation evolution. The first describes the vector potential evolution under the influence of a primordial stochastic magnetic field:

$$\dot{V}_i(\eta, \mathbf{k}) + 2\frac{\dot{a}}{a}V_i(\eta, \mathbf{k}) = -\frac{16\pi G\Pi_i^{(V)}(\mathbf{k})}{a^2 k}, \quad (3.4)$$

where $\Pi_i^{(V)}(\mathbf{k})$ is given by Eq. (2.14) and we neglect the vector anisotropic stress of the plasma, which is in general negligible. The magnetic field source terms $\Pi_i^{(V)}(\mathbf{k})$ and $\Pi_{ij}^{(T)}(\mathbf{k})$ are expressed in terms of present comoving magnetic field amplitudes. Since both of these terms depend on the magnetic field quadratically, the explicit time dependence of the magnetic stress is given by $\Pi(\eta, \mathbf{k}) = \Pi(\mathbf{k})/a^4$. In the absence of the magnetic source term, the homogeneous solution of this equation behaves like $V_i \propto 1/a^2$. The complete solution including the magnetic source is simply

$$V_i(\eta, \mathbf{k}) = -\frac{16\pi G\Pi_i^{(V)}(\mathbf{k})\eta}{a^2 k}. \quad (3.5)$$

During the radiation-dominated epoch we have $a \propto \eta$; a magnetic field therefore causes vector perturbations to decay less rapidly ($1/a$ instead of $1/a^2$) with the Universe’s expansion. The second vector Einstein equation is a constraint that relates the vector potential to the vorticity:

$$-k^2 V_i(\eta, \mathbf{k}) = 16\pi G a^2 (\rho + p) \Omega_i(\eta, \mathbf{k}). \quad (3.6)$$

Vector conservation equations can be obtained via covariant conservation of the stress-energy tensor. Since vector perturbations cannot generate density perturbations, we have

$$\delta_\gamma = \delta_b = 0. \quad (3.7)$$

Before decoupling, photons are coupled to baryons via Thomson scattering. The magnetic field affects the photon-baryon fluid dynamics via the baryons; we therefore introduce the Lorentz force term into the baryon Euler equation. The Euler equations for photons and baryons are respectively [49,53]

$$\dot{\Omega}_{\gamma i} + \dot{\tau}(v_{\gamma i}^{(V)} - v_{bi}^{(V)}) = 0, \quad (3.8)$$

$$\dot{\Omega}_{bi} + \frac{\dot{a}}{a}\Omega_{bi} - \frac{\dot{\tau}}{R}(v_{\gamma i}^{(V)} - v_{bi}^{(V)}) = \frac{L_i^{(V)}(\mathbf{k})}{a^4(\rho_b + p_b)}. \quad (3.9)$$

In the above, $\Omega_{\gamma,b} = \mathbf{v}_{\gamma,b}^{(V)} - \mathbf{V}$ represent vorticities of photons and baryons; $\dot{\tau} = n_e \sigma_T a$ is the differential optical depth where n_e is the free electron density and σ_T is the Thomson cross section; $R \equiv (\rho_b + p_b)/(\rho_\gamma + p_\gamma) \simeq 3\rho_b/4\rho_\gamma$ is the momentum density ratio between baryons and photons; and $L_i^{(V)}$ is the vortical piece of the Lorentz force given by Eq. (2.16). Again, we neglect the small effects due to the vector anisotropic stress of the plasma. This set of vector conservation equations are similar to the one that describes Alfvén waves in Ref. [39] and Eq. (8) of Ref. [50]. Equations (3.4), (3.6), (3.8), and (3.9) are not independent. Using the definitions of R , $L_i^{(V)}$, and the fact that $(\rho_\gamma + p_\gamma) \propto 1/a^4$, and solving the Euler equations in the tight-coupling approximation $v_{\gamma i}^{(V)} \simeq v_{bi}^{(V)}$, we obtain the following approximate solution for the vorticity:

$$\Omega_i(\eta, \mathbf{k}) \simeq \frac{k\Pi_i^{(V)}(\mathbf{k})\eta}{(1+R)(\rho_{\gamma 0} + p_{\gamma 0})}. \quad (3.10)$$

The same result can be obtained using Eqs. (3.5) and (3.6). Before decoupling, dynamics of the plasma is dominated by the photons and $R < 1$. Hence for simplicity, we neglect the Compton drag of baryons in the calculation of the power spectra.

The next step is to introduce two-point correlation functions for the vector potential and the vorticity. Defining their two-point correlation functions as in Eq. (2.17) for the vector $\Pi_i^{(V)}$, and taking ensemble averages of Eqs. (3.5) and (3.10), the rms isotropic spectra for the vector potential and the vorticity are simply

$$V(\eta, k) = -\frac{16\pi G \Pi^{(V)}(k) \eta}{a^2 k}, \quad (3.11)$$

$$\Omega(\eta, k) \simeq \frac{k \Pi^{(V)}(k) \eta}{(1+R)(\rho_{\gamma 0} + p_{\gamma 0})}. \quad (3.12)$$

Vector perturbations induce CMB temperature anisotropies via a Doppler and an integrated Sachs-Wolfe effect [40]:

$$\Theta^{(V)}(\eta_0, \mathbf{k}, \hat{\mathbf{n}}) = -\mathbf{v}^{(V)} \cdot \hat{\mathbf{n}}|_{\eta_{\text{dec}}}^{\eta_0} + \int_{\eta_{\text{dec}}}^{\eta_0} d\eta \dot{\mathbf{V}} \cdot \hat{\mathbf{n}}, \quad (3.13)$$

where η_{dec} represents the conformal time at decoupling. The decaying nature of the vector potential \mathbf{V} implies that most of its contributions toward the integrated Sachs-Wolfe term are around η_{dec} . Neglecting a possible dipole contribution due to $\mathbf{v}^{(V)}$ today, we obtain [40]

$$\Theta^{(V)}(\eta_0, \mathbf{k}, \hat{\mathbf{n}}) \simeq \mathbf{v}^{(V)}(\eta_{\text{dec}}, \mathbf{k}) \cdot \hat{\mathbf{n}} - \mathbf{V}(\eta_{\text{dec}}, \mathbf{k}) \cdot \hat{\mathbf{n}} = \Omega(\eta_{\text{dec}}, \mathbf{k}) \cdot \hat{\mathbf{n}}. \quad (3.14)$$

Vector CMB temperature anisotropies are due to the vorticity at decoupling.

B. Tensor Perturbations

Tensor perturbations of the geometry are described by

$$\delta g_{ij}^{(T)} = 2a^2 h_{ij}, \quad (3.15)$$

where h_{ij} is a symmetric, transverse ($h_{ij} \hat{k}_j = 0$), and traceless ($h_{ii} = 0$) three-tensor. Unlike vector perturbations, tensor perturbations have no gauge freedom.

The tensor Einstein equation that describes the evolution of gravitational waves sourced by a stochastic magnetic field is

$$\ddot{h}_{ij}(\eta, \mathbf{k}) + 2\frac{\dot{a}}{a}\dot{h}_{ij}(\eta, \mathbf{k}) + k^2 h_{ij}(\eta, \mathbf{k}) = 8\pi G \Pi_{ij}^{(T)}(\mathbf{k})/a^2, \quad (3.16)$$

where $\Pi_{ij}^{(T)}(\mathbf{k})$ is given by Eq. (2.19) and as in the case of the vector perturbations, we neglect the tensor anisotropic stress of the plasma, which is in general negligible. Gravitational waves induce CMB temperature anisotropies by causing photons to propagate along perturbed geodesics [52,66]:

$$\Theta^{(T)}(\eta_0, \mathbf{k}, \hat{\mathbf{n}}) \simeq \int_{\eta_{\text{dec}}}^{\eta_0} d\eta \dot{h}_{ij}(\eta, \mathbf{k}) \hat{n}_i \hat{n}_j. \quad (3.17)$$

Our task is, therefore, to obtain the solution for \dot{h}_{ij} . To calculate tensor CMB power spectra, we need to define two-point correlation functions for h_{ij} and \dot{h}_{ij} as in Eq. (2.20) for the tensor $\Pi_{ij}^{(T)}$, with rms isotropic spectra h and \dot{h} respectively. Solutions to the homogeneous equation with $\Pi^{(T)}(k) = 0$ are easily obtained. During the radiation-dominated epoch, $a \propto \eta$ and $h \propto j_0(k\eta)$ or $y_0(k\eta)$, while during the matter-dominated epoch, $a \propto \eta^2$ and $h \propto j_1(k\eta)/k\eta$ or $y_1(k\eta)/k\eta$, where j_1 and y_1 are the usual spherical Bessel functions. Assuming the primordial stochastic magnetic field is generated at η_{in} , a Green function technique yields the following inhomogeneous solution for the radiation-dominated epoch:

$$h(\eta, k) = \frac{2\pi G \Pi^{(T)}(k) z_{\text{eq}}^2 \eta_{\text{eq}}^2}{(3-2\sqrt{2})k\eta} \int_{\eta_{\text{in}}}^{\eta} d\eta' \frac{\sin[k(\eta - \eta')]}{\eta'}, \quad \eta < \eta_{\text{eq}}, \quad (3.18)$$

where η_{eq} denotes the conformal time at matter-radiation equality. The magnetic source term on the right hand side of Eq. (3.16) decays more rapidly with η in the matter-dominated epoch than in the radiation-dominated epoch. An approximate solution, therefore, can be obtained by matching the radiation-dominated inhomogeneous solution of Eq. (3.18) to the matter-dominated homogeneous solutions at equality. Retaining the dominant contribution, we obtain [52]

$$\dot{h}(\eta, k) \simeq 4\pi G \eta_0^2 z_{\text{eq}} \ln\left(\frac{z_{\text{in}}}{z_{\text{eq}}}\right) k \Pi^{(T)}(k) \frac{j_2(k\eta)}{k\eta}, \quad \eta > \eta_{\text{eq}}. \quad (3.19)$$

IV. TEMPERATURE POWER SPECTRA

We employ the total angular momentum representation introduced by Hu and White [53] to compute the CMB power spectra induced by a primordial stochastic magnetic field. By combining intrinsic angular structure with that of the plane-wave spatial dependence, this representation renders a transparent description of CMB anisotropy formation as each moment corresponds directly to an observable angular sky pattern via its integral solution of the Boltzmann equations. The CMB temperature power spectra today is given by Eq. (56) of Ref. [53]:

$$C_l^{\Theta\Theta(X)} = \frac{4}{\pi} \int dk k^2 \frac{\Theta_l^{(X)}(\eta_0, k)}{2l+1} \frac{\Theta_l^{(X)*}(\eta_0, k)}{2l+1}, \quad (4.1)$$

where X stands for V or T , and Θ_l 's are the temperature fluctuation $\Delta T/T$ moments. Note that Eq. (4.1) is larger than the corresponding expression in Ref. [53] by a factor of two as we have already taken into account the fact that both vector and tensor perturbations stimulate two modes individually, corresponding to $m = \pm 1, \pm 2$ respectively in the notation of Ref. [53]. Our strategy is to evaluate the Boltzmann temperature integral solutions to obtain the Θ_l 's due to the vector and tensor perturbations. We then substitute them into Eq. (4.1) to yield the corresponding CMB temperature fluctuations spectra. Though the tensor results are already given in Ref. [52], the vector results derived here are new.

A. Vector Temperature Power Spectra

The Boltzmann temperature integral solution for vector perturbations is given by Eqs. (61) and (74) of Ref. [53]:

$$\frac{\Theta_l^{(V)}(\eta_0, k)}{2l+1} = \int_0^{\eta_0} d\eta e^{-\tau} \left\{ (\dot{\tau} v_b^{(V)} + \dot{V}) j_l^{(1V)}[k(\eta_0 - \eta)] + \dot{\tau} P^{(V)} j_l^{(2V)}[k(\eta_0 - \eta)] \right\}, \quad (4.2)$$

where

$$P^{(V)} = \frac{\sqrt{3}}{9} \frac{k}{\dot{\tau}} v_b^{(V)} \simeq \frac{\sqrt{3}}{9} \frac{k}{\dot{\tau}} \Omega \quad (4.3)$$

is the vector polarization source that is generated when tight coupling breaks down on small scales, where the photon diffusion length and the perturbation wavelength become comparable. The approximation in Eq. (4.3) is obtained using Eq. (3.3) and noting that Ω dominates V at decoupling [cf. Eqs. (3.11) and (3.12)] for $k > 0.0053 \text{ Mpc}^{-1}$, which results in V contributing negligibly compared to Ω upon integrating over k 's to obtain the vector temperature power spectra in Eq. (4.1). Unlike scalar perturbations, vector perturbations cannot produce compressional modes due to the lack of pressure support. In the usual case of vector perturbations in cosmological fluids without a magnetic field, tight-coupling expansion of photon and baryon Euler equations give $v_b^{(V)} \approx V$, resulting in the vector polarization source being dependent on the vector potential instead (see Eq. (94) of Ref. [53]). A primordial stochastic magnetic field thus enhances vector polarization by sourcing the vorticity. The vector temperature radial functions $j_l^{(1V)}$ and $j_l^{(2V)}$, which describe how distant sources contribute, are given by Eq. (15) of Ref. [53]:

$$\begin{aligned} j_l^{(1V)}(x) &= \sqrt{\frac{l(l+1)}{2}} \frac{j_l(x)}{x}, \\ j_l^{(2V)}(x) &= \sqrt{\frac{3l(l+1)}{2}} \frac{d}{dx} \left(\frac{j_l(x)}{x} \right). \end{aligned} \quad (4.4)$$

The optical depth between η and η_0 is defined as $\tau(\eta) \equiv \int_\eta^{\eta_0} d\eta' \dot{\tau}(\eta')$, thus $d\tau/d\eta = -\dot{\tau}$. Integrating Eq. (4.2) by parts using $de^{-\tau}/d\eta = \dot{\tau}e^{-\tau}$ and $j_l^{(2V)}(x) = \sqrt{3}(j_l^{(1V)}(x))'$ and Eqs. (3.3) and (4.3), we obtain

$$\frac{\Theta_l^{(V)}(\eta_0, k)}{2l+1} = \int_0^{\eta_0} d\eta \dot{\tau}e^{-\tau} \left\{ \Omega j_l^{(1V)}[k(\eta_0 - \eta)] + \frac{\sqrt{3}k}{9\dot{\tau}}(\Omega + 3V)j_l^{(2V)}[k(\eta_0 - \eta)] \right\}. \quad (4.5)$$

For the usual vector perturbations without a magnetic field, the term proportional to $j_l^{(1V)}$ is strongly suppressed since $v_b^{(V)} \approx V$ at decoupling [53] and hence $\Omega \simeq 0$ as mentioned above. Here we have a primordial stochastic magnetic field sourcing Ω ; the term proportional to $j_l^{(2V)}$ is then suppressed relative to the term proportional to $j_l^{(1V)}$ due to the factor $k/\dot{\tau}$. Moreover, $j_l^{(2V)}$ has less angular power compared to $j_l^{(1V)}$ (see Fig. 3 of Ref. [53]). Thus to simplify the calculation, we consider only the term proportional to $j_l^{(1V)}$ in computing the vector temperature integral solution. Including the small corrections due to the angular dependence of polarization from the term proportional to $P^{(V)}j_l^{(2V)}$ will give an additional 10% contribution toward our final estimate of the vector temperature power spectra, whereas including the vector potential will only give a negligible contribution of $\ll 1\%$. The combination $\dot{\tau}e^{-\tau}$ is the conformal visibility function, which represents the probability that a photon last scattered within $d\eta$ of η and hence is sharply peaked at the decoupling period. We can therefore approximate the vector temperature integral solution as

$$\frac{\Theta_l^{(V)}(\eta_0, k)}{2l+1} \simeq \sqrt{\frac{l(l+1)}{2}} \Omega(\eta_{\text{dec}}, k) \frac{j_l(k\eta_0)}{k\eta_0}, \quad (4.6)$$

using Eq. (4.4) and the fact that $\eta_0 \gg \eta_{\text{dec}}$. The vector CMB temperature anisotropies are due to the vorticity at decoupling, as also illustrated by Eq. (3.14). Substituting Eq. (4.6) into the CMB temperature power spectrum expression of Eq. (4.1), using Eqs. (3.12), (2.18), and neglecting the baryon inertia, we obtain

$$C_l^{\Theta\Theta(V)} = (2\pi)^{2n+11} l(l+1) \left(\frac{\eta_{\text{dec}}}{\eta_0} \right)^2 \frac{v_A^4 \eta_0^2}{\Gamma^2 \left(\frac{n+3}{2} \right) (2n+3)(k_D \eta_0)^3} \int_0^{k_D} dk k \left[1 + \frac{n}{n+3} \left(\frac{k}{k_D} \right)^{2n+3} \right] J_{l+1/2}^2(k\eta_0), \quad (4.7)$$

where $v_A = B_0/[4\pi(\rho_{\gamma 0} + p_{\gamma 0})]^{1/2} = 3.77 \times 10^{-4} (B_0/10^{-9} \text{ G})$ is the Alfvén velocity.

Depending on whether $n > -3/2$ or $-3 < n < -3/2$, we retain only the corresponding dominant term in Eq. (4.7). First consider the case $n > -3/2$, where the vorticity source becomes approximately white noise (independent of k), resulting in $|\Pi^{(V)}(k)|^2$ being dependent on k_D . To obtain an analytic estimate of the integral $\int_0^{k_D} dk k J_{l+1/2}^2(k\eta_0)$, consider the more general integral $\int_0^{x_D} dx x^p J_l^2(x)$ for some $p \geq 0$. Since $J_l(x)$ only begins to contribute to the integral significantly when $x \gtrsim l$, in this limit, we employ in the integral the $J_l(x)$ asymptotic expansion for large argument [67]: $J_l(x) \sim \sqrt{2/(\pi x)} \cos[x - (2l+1)\pi/4]$. Approximating the oscillations by a factor of one half then gives

$$\int_0^{x_D} dx x^p J_l^2(x) \simeq \int_l^{x_D} dx x^p J_l^2(x) \simeq \begin{cases} \frac{x_D^p - l^p}{p\pi}, & p > 0; \\ \frac{1}{\pi} \ln \left(\frac{x_D}{l} \right), & p = 0. \end{cases} \quad (4.8)$$

In the limit $x_D \gg l$, the approximation is good to a few percent for $p \geq 1$ and within 20% for $0 \leq p < 1$. The integral $\int_0^{k_D} dk k J_{l+1/2}^2(k\eta_0)$ corresponds to the case $p = 1$; using $k_D \eta_0 \gg l$ (easily satisfied for $l \lesssim 500$) and keeping only the highest-order term in l , we obtain the vector CMB temperature power spectrum for $n > -3/2$:

$$l^2 C_l^{\Theta\Theta(V)} = 2(2\pi)^{2n+10} \left(\frac{\eta_{\text{dec}}}{\eta_0} \right)^2 \frac{v_A^4 l^4}{\Gamma^2 \left(\frac{n+3}{2} \right) (2n+3)(k_D \eta_0)^2}, \quad n > -3/2. \quad (4.9)$$

For $-3 < n < -3/2$, the needed integral is $\int_0^{k_D} dk k^{2n+4} J_{l+1/2}^2(k\eta_0)$. We must consider three cases depending on whether the exponent $2n+4$ is greater than, equal to, or less than zero. For $-2 < n < -3/2$, using Eq. (4.8) for $p = 2n+4$, we obtain

$$l^2 C_l^{\Theta\Theta(V)} = (2\pi)^{2n+10} \left(\frac{\eta_{\text{dec}}}{\eta_0} \right)^2 \frac{v_A^4 n l^4}{\Gamma^2 \left(\frac{n+3}{2} \right) (2n+3)(n+2)(n+3)(k_D \eta_0)^2} \left[1 - \left(\frac{l}{k_D \eta_0} \right)^{2n+4} \right], \quad -2 < n < -3/2. \quad (4.10)$$

For $n = -2$, again using Eq. (4.8) for $p = 0$, we obtain

$$l^2 C_l^{\Theta\Theta(V)} = 8(2\pi)^5 \left(\frac{\eta_{\text{dec}}}{\eta_0} \right)^2 \frac{v_A^4}{(k_D \eta_0)^2} \ln \left(\frac{k_D \eta_0}{l} \right) l^4, \quad n = -2. \quad (4.11)$$

For $-3 < n < -2$, the dominant contribution to the integral $\int_0^{k_D} dk k^{2n+4} J_{l+1/2}^2(k\eta_0)$ is from long wavelengths $k \rightarrow 0$ and hence the resulting vector CMB temperature power spectrum is independent of k_D . This integral can be evaluated analytically by using 6.574.2 of Ref. [68],

$$\int_0^\infty dk J_p(\alpha k) J_q(\alpha k) k^{-\beta} = \frac{\alpha^{\beta-1} \Gamma(\beta) \Gamma\left(\frac{p+q-\beta+1}{2}\right)}{2^\beta \Gamma\left(\frac{-p+q+\beta+1}{2}\right) \Gamma\left(\frac{p+q+\beta+1}{2}\right) \Gamma\left(\frac{p-q+\beta+1}{2}\right)}, \quad \text{Re}(p+q+1) > \text{Re}\beta > 0, \alpha > 0; \quad (4.12)$$

and 8.335.1 of Ref. [68],

$$\Gamma(2x) = \frac{2^{2x-1}}{\sqrt{\pi}} \Gamma(x) \Gamma\left(x + \frac{1}{2}\right); \quad (4.13)$$

we finally obtain

$$l^2 C_l^{\Theta\Theta(V)} = \frac{(2\pi)^{2n+10}}{2^{2n+4}} \left(\frac{\eta_{\text{dec}}}{\eta_0} \right)^2 \frac{\Gamma^2(-n-1)}{\Gamma(-2n-3) \Gamma^2\left(\frac{n+3}{2}\right)} \frac{-v_A^4 n l^{2n+8}}{(2n+3)(n+2)(n+3)(k_D \eta_0)^{2n+6}}, \quad -3 < n < -2. \quad (4.14)$$

Recall that the apparent dependence on k_D above is due to the fact that v_A^4/k_D^{2n+6} is a constant, being proportional to the square of the magnetic power spectrum normalization. The temperature power spectrum of each case above has the same l and k_D dependence as the corresponding spectrum induced by a primordial homogeneous magnetic field [40] (the correspondence between the spectral index of Ref. [40] and ours is $n \rightarrow 2n+3$). For the sake of completeness, we note that the vector potential contribution arising from the $j_l^{(2V)}$ term in Eq. (4.5) will induce temperature power spectra $l^2 C_l^{\Theta\Theta(V)} \propto l^3$ for $n > -3/2$ and $l^2 C_l^{\Theta\Theta(V)} \propto l^{2n+6}$ for $-3 < n < -3/2$.

We now consider the case $n = -3/2$ and show that this apparent singularity is removable by considering both terms of the vector isotropic spectrum in Eq. (2.18). In the limit $n = -3/2 + \varepsilon$, we have

$$|\Pi^{(V)}(k)|^2 \simeq \frac{(2\pi)^6}{4} \frac{B_0^4}{\Gamma^2\left(\frac{3}{4}\right) k_D^3} \frac{1}{2\varepsilon} \left[1 - \left(1 - \frac{2\varepsilon}{3}\right) \left(1 + \frac{2\varepsilon}{3}\right)^{-1} \left(\frac{k}{k_D}\right)^{2\varepsilon} \right]. \quad (4.15)$$

In the neighborhood of $n = -3/2$, the source contribution peaks at small scales where $k \simeq k_D$. Upon expanding the expression within the square bracket to $\mathcal{O}(\varepsilon)$ and using the small- x expansion $\ln(1+x) \sim x$ for $x \equiv -(k_D - k)/k_D$, we obtain

$$|\Pi^{(V)}(k)|^2 \simeq \frac{(2\pi)^6}{4} \frac{B_0^4}{\Gamma^2\left(\frac{3}{4}\right) k_D^3} \left(\frac{5}{3} - \frac{k}{k_D}\right), \quad n \approx -3/2. \quad (4.16)$$

The same result can be obtained via direct substitution of $n = -3/2$ in Eqs. (A9) to (A11). Using Eqs. (4.16) and (4.8) for $p = 1$ and 2, a similar calculation as in Eq. (4.9) then gives

$$l^2 C_l^{\Theta\Theta(V)} = \frac{7}{3} (2\pi)^7 \left(\frac{\eta_{\text{dec}}}{\eta_0} \right)^2 \frac{v_A^4 l^4}{\Gamma^2\left(\frac{3}{4}\right) (k_D \eta_0)^2}, \quad n \approx -3/2, \quad (4.17)$$

thus showing that the singularity at $n = -3/2$ is indeed removable. For the rest of the paper, we will not produce explicit power spectrum expressions for the case $n = -3/2$. Readers who are interested can easily derive the corresponding results via a straightforward extension of the calculation outlined above.

B. Tensor Temperature Power Spectra

The Boltzmann temperature integral solution for tensor perturbations is given by Eqs. (61) and (74) of Ref. [53]:

$$\frac{\Theta_l^{(T)}(\eta_0, k)}{2l+1} = \int_0^{\eta_0} d\eta e^{-\tau} [\dot{\tau} P^{(T)} - \dot{h}] j_l^{(2T)}[k(\eta_0 - \eta)], \quad (4.18)$$

where

$$P^{(T)} = -\frac{1}{3} \frac{\dot{h}}{\dot{\tau}} \quad (4.19)$$

is the tensor polarization source and $j_l^{(2T)}$ is the tensor temperature radial function given by Eq. (15) of Ref. [53]:

$$j_l^{(2T)}(x) = \sqrt{\frac{3}{8} \frac{(l+2)!}{(l-2)!}} \frac{j_l(x)}{x^2}. \quad (4.20)$$

Using Eq. (3.19) and defining $x \equiv k\eta$ and $x_0 \equiv k\eta_0$, we approximate the tensor temperature integral solution as

$$\frac{\Theta_l^{(T)}(\eta_0, k)}{2l+1} \simeq -2\pi \sqrt{\frac{8}{3} \frac{(l+2)!}{(l-2)!}} \left[G\eta_0^2 z_{\text{eq}} \ln\left(\frac{z_{\text{in}}}{z_{\text{eq}}}\right) \right] \Pi^{(T)}(k) \int_0^{x_0} dx \frac{j_2(x)}{x} \frac{j_l(x_0 - x)}{(x_0 - x)^2}. \quad (4.21)$$

The integral above can be numerically approximated as in Eq. (19) of Ref. [52],

$$\begin{aligned} \int_0^{x_0} dx \frac{j_2(x)}{x} \frac{j_l(x_0 - x)}{(x_0 - x)^2} &= \frac{\pi}{2} \int_0^{x_0} dx \frac{J_{5/2}(x)}{x^{3/2}} \frac{J_{l+1/2}(x_0 - x)}{(x_0 - x)^{5/2}} \\ &\simeq \frac{7\pi}{20} \sqrt{l} \int_0^{x_0} dx \frac{J_{5/2}(x)}{x} \frac{J_{l+1/2}(x_0 - x)}{(x_0 - x)^3} \\ &\simeq \frac{7\pi}{50} \sqrt{\frac{3l}{2}} \frac{J_{l+3}(x_0)}{x_0^3}, \end{aligned} \quad (4.22)$$

where in going from the second to the third line, we have inserted a factor of $\sqrt{3/2}$ for better numerical agreement and used 6.581.2 of Ref. [68]:

$$\begin{aligned} \int_0^\alpha dx x^{\beta-1} (\alpha - x)^{-1} J_p(x) J_q(\alpha - x) &= \frac{2^\beta}{\alpha q} \sum_{m=0}^{\infty} \frac{(-1)^m \Gamma(\beta + p + m) \Gamma(\beta + m)}{m! \Gamma(\beta) \Gamma(p + m + 1)} (\beta + p + q + 2m) J_{\beta+p+q+2m}(\alpha), \\ \text{Re } (\beta + p) &> 0, \text{ Re } q > 0. \end{aligned} \quad (4.23)$$

Numerical evaluation shows that the approximation in the second line of Eq. (4.22) is good to 10%. Substituting Eq. (4.22) into Eq. (4.21) yields

$$\frac{\Theta_l^{(T)}(\eta_0, k)}{2l+1} \simeq -\frac{7}{50} (2\pi)^2 \sqrt{\frac{l(l+2)!}{(l-2)!}} \left[G\eta_0^2 z_{\text{eq}} \ln\left(\frac{z_{\text{in}}}{z_{\text{eq}}}\right) \right] \Pi^{(T)}(k) \frac{J_{l+3}(k\eta_0)}{(k\eta_0)^3}. \quad (4.24)$$

Using Eqs. (2.22), (4.1), and (4.24), we obtain

$$\begin{aligned} C_l^{\Theta\Theta(T)} &= \frac{49}{2500} (2\pi)^{2n+12} l^2 (l-1)(l+1)(l+2) \left[G\eta_0^2 z_{\text{eq}} \ln\left(\frac{z_{\text{in}}}{z_{\text{eq}}}\right) \right]^2 \frac{B_0^4 k_D^3}{\Gamma^2\left(\frac{n+3}{2}\right) (2n+3)(k_D\eta_0)^6} \\ &\times \int_0^{k_D} dk k^{-4} \left[1 + \frac{n}{n+3} \left(\frac{k}{k_D} \right)^{2n+3} \right] J_{l+3}^2(k\eta_0). \end{aligned} \quad (4.25)$$

For $n > -3/2$, the gravitational wave source is k_D -dependent, and the resulting temperature fluctuation spectrum possesses the well-known behavior $l^2 C_l \propto l^3$. The integral $\int_0^{k_D} dk k^{-4} J_{l+3}^2(k\eta_0)$ can be evaluated using Eq. (4.12); retaining only the highest-order term in l , we obtain

$$l^2 C_l^{\Theta\Theta(T)} = \frac{49}{1875} (2\pi)^{2n+11} \left[G\eta_0^2 z_{\text{eq}} \ln \left(\frac{z_{\text{in}}}{z_{\text{eq}}} \right) \right]^2 \frac{B_0^4}{\Gamma^2 \left(\frac{n+3}{2} \right) (2n+3)} \left(\frac{l}{k_D \eta_0} \right)^3, \quad n > -3/2. \quad (4.26)$$

For $-3 < n < -3/2$, a similar calculation gives

$$l^2 C_l^{\Theta\Theta(T)} = 2^{2n-3} \frac{49}{625} (2\pi)^{2n+12} \left[G\eta_0^2 z_{\text{eq}} \ln \left(\frac{z_{\text{in}}}{z_{\text{eq}}} \right) \right]^2 \frac{B_0^4}{\Gamma^2 \left(\frac{n+3}{2} \right)} \frac{\Gamma(1-2n)}{\Gamma^2(1-n)} \frac{n}{(2n+3)(n+3)} \left(\frac{l}{k_D \eta_0} \right)^{2n+6}, \quad -3 < n < -3/2. \quad (4.27)$$

Again, as in Eq. (4.14) of the vector case, the illusory dependence on k_D here is because B_0^4/k_D^{2n+6} is proportional to the square of the magnetic power spectrum normalization. Equivalent tensor perturbation results are given in Ref. [52].

V. POLARIZATION POWER SPECTRA

Polarization of the CMB comes in two flavors: E-type and B-type with electric $(-1)^l$ and magnetic $(-1)^{l+1}$ parities respectively [69,70]. Physically, they represent polarization patterns rotated by $\pi/4$ due to the interchanging of Q and U Stokes parameters. Vector and tensor perturbations induce both types of polarizations. Scalar perturbations, however, cannot generate B-type polarization due to azimuthal symmetry. A detection of the B-type polarization from future high sensitivity CMB polarization measurements therefore would provide compelling evidence for vector and/or tensor contributions. Similar to the CMB temperature power spectra of Eq. (4.1), the E-type and B-type polarization power spectra are respectively

$$C_l^{EE(X)} = \frac{4}{\pi} \int dk k^2 \frac{E_l^{(X)}(\eta_0, k)}{2l+1} \frac{E_l^{(X)*}(\eta_0, k)}{2l+1}, \quad (5.1)$$

$$C_l^{BB(X)} = \frac{4}{\pi} \int dk k^2 \frac{B_l^{(X)}(\eta_0, k)}{2l+1} \frac{B_l^{(X)*}(\eta_0, k)}{2l+1}, \quad (5.2)$$

where X stands for V or T . The correspondence between notations of Ref. [53] and ours for polarization moments are $E_l^{(\pm 1)} \rightarrow E_l^{(V)}$ and $B_l^{(\pm 1)} \rightarrow \pm B_l^{(V)}$, and similarly for the tensor perturbations.

A. Vector Polarization Power Spectra

1. E-type Polarization

The E-type polarization integral solution for vector perturbations is [53]

$$\frac{E_l^{(V)}(\eta_0, k)}{2l+1} = -\sqrt{6} \int_0^{\eta_0} d\eta \dot{\tau} e^{-\tau} P^{(V)} \epsilon_l^{(V)}[k(\eta_0 - \eta)], \quad (5.3)$$

where

$$\epsilon_l^{(V)}(x) = \frac{1}{2} \sqrt{(l-1)(l+2)} \left[\frac{j_l(x)}{x^2} + \frac{j'_l(x)}{x} \right] \quad (5.4)$$

is the vector E-type polarization radial function given by Eq. (17) of Ref. [53]. Using Eq. (4.3) for $P^{(V)}$ and the spherical Bessel function recurrence relation [67]

$$\frac{l}{x} j_l(x) - j'_l(x) = j_{l+1}(x), \quad (5.5)$$

we approximate the vector E-type polarization integral solution as in Eq. (4.6):

$$\frac{E_l^{(V)}(\eta_0, k)}{2l+1} \simeq -\sqrt{\frac{(l-1)(l+2)}{18}} \frac{k}{\dot{\tau}(\eta_{\text{dec}})} \Omega(\eta_{\text{dec}}, k) \left[(l+1) \frac{j_l(k\eta_0)}{(k\eta_0)^2} - \frac{j_{l+1}(k\eta_0)}{k\eta_0} \right]. \quad (5.6)$$

The value of $\dot{\tau}(\eta_{\text{dec}})$ can be estimated as follows. During the recombination epoch $800 < z < 1200$, the differential optical depth can be parametrized as [71]

$$\dot{\tau}(z) = \Omega_b^{c_1} \left(\frac{c_2}{1000} \right) \left(\frac{z}{1000} \right)^{c_2-1} \frac{\dot{a}}{a} (1+z), \quad (5.7)$$

where $c_1 = 0.43$ and $c_2 = 16 + 1.8 \ln \Omega_b$. Taking $\Omega_b = 0.05$ and $z_{\text{dec}} = 1100$, we obtain an analytic estimate of $\dot{\tau}(\eta_{\text{dec}}) \simeq 16/\eta_{\text{dec}}$ (see also Appendix B of Ref. [40]). Substituting Eq. (5.6) into (5.1), using Eqs. (3.12) and (2.18), and neglecting the baryon inertia, we obtain

$$C_l^{EE(V)} = \frac{(2\pi)^{2n+11}}{9} (l-1)(l+2) \left(\frac{\eta_{\text{dec}}}{\eta_0} \right)^2 \frac{v_A^4 \eta_0^4}{\Gamma^2 \left(\frac{n+3}{2} \right) (2n+3)(k_D \eta_0)^3} \times \int_0^{k_D} dk k^3 \left(\frac{k}{k_*} \right)^2 \left[1 + \frac{n}{n+3} \left(\frac{k}{k_D} \right)^{2n+3} \right] \left[(l+1) \frac{J_{l+1/2}(k\eta_0)}{(k\eta_0)^2} - \frac{J_{l+3/2}(k\eta_0)}{k\eta_0} \right]^2, \quad (5.8)$$

where we have defined $k_* \equiv \dot{\tau}(\eta_{\text{dec}})$. For $k < k_*$ at decoupling, in the tight-coupling limit, the vector temperature quadrupole moment $\Theta_2^{(V)}$ is suppressed relative to the dipole moment $\Theta_1^{(V)}$ by the factor $(4\sqrt{3}/9)k/k_*$ (see Eq. (90) of Ref. [53]). For $k \geq k_*$ at decoupling, in order not to overproduce polarization fluctuations, we assume all the dipoles have already free-streamed into quadrupoles, hence we discard the factor k/k_* and simply take $\Theta_2^{(V)} \simeq (4\sqrt{3}/9)\Theta_1^{(V)}$. The k integral in Eq. (5.8) therefore formally represents $\int_0^{k_D} dk k^3 (k/k_*)^2 \equiv \int_0^{k_*} dk k^3 (k/k_*)^2 + \int_{k_*}^{k_D} dk k^3$.

A numerical evaluation shows that the dominant contribution toward $C_l^{EE(V)}$ for $n \geq -5/2$ comes from the term proportional to $J_{l+3/2}^2(k\eta_0)$. The cross term proportional to $J_{l+1/2}(k\eta_0)J_{l+3/2}(k\eta_0)$ is difficult to evaluate analytically; thus to simplify the calculation, we will consider only the term proportional to $J_{l+3/2}^2(k\eta_0)$ for both $n > -3/2$ and $-3 < n < -3/2$, and will note in each case how good is this approximation.

For $n > -3/2$, the dominant term is the integral $\int_{k_*}^{k_D} dk k^3 J_{l+3/2}^2(k\eta_0)/(k\eta_0)^2$. Using a similar approximation as in Eq. (4.8) for $p = 1$ and the fact that $k_D \gg k_*$, we obtain

$$l^2 C_l^{EE(V)} = \frac{2}{9} (2\pi)^{2n+10} \left(\frac{\eta_{\text{dec}}}{\eta_0} \right)^2 \frac{v_A^4 l^4}{\Gamma^2 \left(\frac{n+3}{2} \right) (2n+3)(k_D \eta_0)^2}, \quad n > -3/2. \quad (5.9)$$

Comparing to the numerical evaluation of Eq. (5.8) shows that our approximation is good to within 5%.

For $-3 < n < -3/2$, we need to evaluate

$$\int_0^{k_D} dk k^{2n+4} \left(\frac{k}{k_*} \right)^2 J_{l+3/2}^2(k\eta_0) \equiv \int_0^{k_*} dk k^{2n+4} \left(\frac{k}{k_*} \right)^2 J_{l+3/2}^2(k\eta_0) + \int_{k_*}^{k_D} dk k^{2n+4} J_{l+3/2}^2(k\eta_0). \quad (5.10)$$

Since the second integral on the rhs always dominates the first for $-5/2 \leq n < -3/2$, as in the case of the vector temperature power spectra in Sec. IV A, we then consider three cases depending on whether its exponent $2n+4$ is greater than, equal to, or less than zero in this regime. For $-2 < n < -3/2$, these two integrals can be well-approximated by $k_*^{2n+4}/[2\pi(n+3)\eta_0]$ and $(k_D^{2n+4} - k_*^{2n+4})/[2\pi(n+2)\eta_0]$ respectively (as with Eq. (5.9)). Therefore we obtain

$$l^2 C_l^{EE(V)} = \frac{(2\pi)^{2n+10}}{9} \left(\frac{\eta_{\text{dec}}}{\eta_0} \right)^2 \frac{v_A^4 n l^4}{\Gamma^2 \left(\frac{n+3}{2} \right) (2n+3)(n+2)(n+3)^2 (k_D \eta_0)^2} \left[n+3 - \left(\frac{k_*}{k_D} \right)^{2n+4} \right], \quad -2 < n < -3/2. \quad (5.11)$$

Numerical evaluation of Eq. (5.8) shows that our approximation is good to a few percent for $l \lesssim 400$ and overestimates by less than 30% for $400 \lesssim l \leq 500$. This overestimation is because the cross term proportional to $J_{l+1/2}(k\eta_0)J_{l+3/2}(k\eta_0)$ in Eq. (5.8) is becoming important. For $n = -2$, the two integrals on the rhs of Eq. (5.10) can be approximated by $1/(2\pi\eta_0)$ and $\ln(k_D/k_*)/(\pi\eta_0)$ respectively. We then obtain

$$l^2 C_l^{EE(V)} = \frac{4}{9} (2\pi)^5 \left(\frac{\eta_{\text{dec}}}{\eta_0} \right)^2 \frac{v_A^4}{(k_D \eta_0)^2} \left[1 + 2 \ln \left(\frac{k_D}{k_*} \right) \right] l^4, \quad n = -2. \quad (5.12)$$

Since the magnitude of the neglected terms proportional to $J_{l+1/2}^2(k\eta_0)$ and $J_{l+1/2}(k\eta_0)J_{l+3/2}(k\eta_0)$ in Eq. (5.8) are getting larger as n decreases, our approximation is becoming worse, as expected. For $l \lesssim 400$, it is good to a few

percent; whereas for $400 \lesssim l \leq 500$, it overestimates by at most 30–40%. For $-5/2 \leq n < -2$, even though the exponent $2n + 4$ of the second integral on the right side of Eq. (5.10) is now negative, this integral can be well-approximated by $(k_D^{2n+4} - k_*^{2n+4})/[2\pi(n+2)\eta_0]$. As in Eq. (4.8), this approximation is obtained via employing the Bessel function asymptotic expansion for large argument, which is justified since $k\eta_0 \gtrsim l$ for $k_* \leq k \leq k_D$. The resulting power spectrum expression is then formally identical to that of the case $-2 < n < -3/2$:

$$l^2 C_l^{EE(V)} = \frac{(2\pi)^{2n+10}}{9} \left(\frac{\eta_{\text{dec}}}{\eta_0} \right)^2 \frac{v_A^4 nl^4}{\Gamma^2 \left(\frac{n+3}{2} \right) (2n+3)(n+2)(n+3)^2 (k_D \eta_0)^2} \left[n + 3 - \left(\frac{k_*}{k_D} \right)^{2n+4} \right], \quad -5/2 \leq n < -2. \quad (5.13)$$

Here, our estimation is good to within a factor of two; accuracy decreases as n decreases and/or l increases. Again, this is because we have retained only one of the three terms in Eq. (5.8) when calculating the power spectrum.

Finally we consider the case $-3 < n < -5/2$. Since $0 < 2n+6 < 1$, the first integral on the rhs of Eq. (5.10) is better approximated by $k_*^{2n+4}[1 - (l/k_*\eta_0)^{2n+6}]/[2\pi(n+3)\eta_0]$ whereas again we can approximate the second integral by $(k_D^{2n+4} - k_*^{2n+4})/[2\pi(n+2)\eta_0]$. We obtain

$$l^2 C_l^{EE(V)} = \frac{(2\pi)^{2n+10}}{9} \left(\frac{\eta_{\text{dec}}}{\eta_0} \right)^2 \frac{v_A^4 nl^4}{\Gamma^2 \left(\frac{n+3}{2} \right) (2n+3)(n+2)(n+3)^2 (k_D \eta_0)^2} \times \left\{ n + 3 - \left(\frac{k_*}{k_D} \right)^{2n+4} \left[1 + (n+2) \left(\frac{l}{k_* \eta_0} \right)^{2n+6} \right] \right\}, \quad -3 < n < -5/2. \quad (5.14)$$

Our approximation here is slightly better than the case $-5/2 \leq n < -2$. We overestimate by at most 60%; again, accuracy decreases as n decreases and/or l increases. Since the dominant term within the power spectrum for cases $-5/2 \leq n < -2$ and $-3 < n < -5/2$ is proportional to $(1/k_D)^{2n+6}$, these two cases do not depend explicitly on the cutoff scale because $v_A^4 \propto k_D^{2n+6}$. As we will see, the same comment also applies to the corresponding cases of vector B-type polarization and cross-correlation.

2. B-type Polarization

The B-type polarization integral solution for vector perturbations is [53]

$$\frac{B_l^{(V)}(\eta_0, k)}{2l+1} = -\sqrt{6} \int_0^{\eta_0} d\eta \dot{\tau} e^{-\tau} P^{(V)} \beta_l^{(V)}[k(\eta_0 - \eta)], \quad (5.15)$$

where

$$\beta_l^{(V)}(x) = \frac{1}{2} \sqrt{(l-1)(l+2)} \frac{j_l(x)}{x} \quad (5.16)$$

is the vector B-type polarization radial function. Using the same approximation in Eq. (5.15) as in Eq. (4.6), we obtain

$$\frac{B_l^{(V)}(\eta_0, k)}{2l+1} \simeq -\sqrt{\frac{(l-1)(l+2)}{18}} \frac{k}{\dot{\tau}(\eta_{\text{dec}})} \Omega(\eta_{\text{dec}}, k) \frac{j_l(k\eta_0)}{k\eta_0}, \quad (5.17)$$

which upon substituting into Eq. (5.2), using Eqs. (3.12) and (2.18), and neglecting the baryon inertia, yields

$$C_l^{BB(V)} = \frac{(2\pi)^{2n+11}}{9} (l-1)(l+2) \left(\frac{\eta_{\text{dec}}}{\eta_0} \right)^2 \frac{v_A^4 \eta_0^4}{\Gamma^2 \left(\frac{n+3}{2} \right) (2n+3)(k_D \eta_0)^3} \times \int_0^{k_D} dk k^3 \left(\frac{k}{k_*} \right)^2 \left[1 + \frac{n}{n+3} \left(\frac{k}{k_D} \right)^{2n+3} \right] \frac{J_{l+1/2}^2(k\eta_0)}{(k\eta_0)^2}, \quad (5.18)$$

where again we have defined $k_* \equiv \dot{\tau}(\eta_{\text{dec}})$. Except for the order of the Bessel function, Eq. (5.18) is identical to the dominant term retained in the vector E-type polarization power spectrum expression given in Eq. (5.8). Therefore the

resulting power spectra for all cases are approximately equal to the corresponding vector E-type polarization power spectra, Eq. (5.9) and Eqs. (5.11) to (5.14).

Since we do not have any neglected terms here as in the case of vector E-type polarization power spectra, our accuracy is good to the quality of analytic approximations. For $n \geq -5/2$, our approximation is good to within 15%, with improving accuracy as n increases. For $-3 < n < -5/2$, our approximation tends to underestimate, but always good to within 50%.

B. Tensor Polarization Power Spectra

1. E-type Polarization

The E-type polarization integral solution for tensor perturbations is [53]

$$\frac{E_l^{(T)}(\eta_0, k)}{2l+1} = -\sqrt{6} \int_0^{\eta_0} d\eta \dot{\tau} e^{-\tau} P^{(T)} \epsilon_l^{(T)}[k(\eta_0 - \eta)], \quad (5.19)$$

where $P^{(T)}$ is given by Eq. (4.19), and

$$\epsilon_l^{(T)}(x) = \frac{1}{4} \left[-j_l(x) + j_l''(x) + 2 \frac{j_l(x)}{x^2} + 4 \frac{j_l'(x)}{x} \right] \quad (5.20)$$

is the tensor E-type polarization radial function. Using Eqs. (3.19) and (5.5) and the spherical Bessel function recurrence relation [67]

$$\frac{l+1}{x} j_l(x) + j_l'(x) = j_{l-1}(x), \quad (5.21)$$

and defining $x \equiv k\eta$ and $x_0 \equiv k\eta_0$, we approximate the tensor E-type polarization integral solution as

$$\begin{aligned} \frac{E_l^{(T)}(\eta_0, k)}{2l+1} &\simeq \frac{2\pi}{\sqrt{6}} \left[G\eta_0^2 z_{\text{eq}} \ln \left(\frac{z_{\text{in}}}{z_{\text{eq}}} \right) \right] \Pi^{(T)}(k) \\ &\times \int_0^{x_0} dx \frac{j_2(x)}{x} \left\{ \left[-2 + \frac{(l+1)(l+2)}{(x_0 - x)^2} \right] j_l(x_0 - x) - \frac{2}{x_0 - x} j_{l+1}(x_0 - x) \right\}. \end{aligned} \quad (5.22)$$

A similar manipulation as in Eq. (4.22) gives

$$\frac{E_l^{(T)}(\eta_0, k)}{2l+1} \simeq -\frac{7}{100} (2\pi)^2 \sqrt{l} \left[G\eta_0^2 z_{\text{eq}} \ln \left(\frac{z_{\text{in}}}{z_{\text{eq}}} \right) \right] \frac{\Pi^{(T)}(k)}{k\eta_0} \left\{ \left[1 - \frac{l^2}{2(k\eta_0)^2} \right] J_{l+3}(k\eta_0) + \frac{J_{l+4}(k\eta_0)}{k\eta_0} \right\}. \quad (5.23)$$

Substituting Eq. (5.23) into Eq. (5.1) and using Eq. (2.22), we obtain

$$\begin{aligned} C_l^{EE(T)} &= \frac{49}{10000} (2\pi)^{2n+12} l \left[G\eta_0^2 z_{\text{eq}} \ln \left(\frac{z_{\text{in}}}{z_{\text{eq}}} \right) \right]^2 \frac{B_0^4 \eta_0}{\Gamma^2 \left(\frac{n+3}{2} \right) (2n+3)(k_D \eta_0)^3} \\ &\times \int_0^{k_D} dk \left[1 + \frac{n}{n+3} \left(\frac{k}{k_D} \right)^{2n+3} \right] \left\{ \left[1 - \frac{l^2}{2(k\eta_0)^2} \right] J_{l+3}(k\eta_0) + \frac{J_{l+4}(k\eta_0)}{k\eta_0} \right\}^2. \end{aligned} \quad (5.24)$$

For $n > -3/2$, using Eqs. (4.8) and (4.12) and keeping only the highest-order terms in l gives

$$l^2 C_l^{EE(T)} = \frac{49}{5000} (2\pi)^{2n+11} \left[G\eta_0^2 z_{\text{eq}} \ln \left(\frac{z_{\text{in}}}{z_{\text{eq}}} \right) \right]^2 \frac{B_0^4}{\Gamma^2 \left(\frac{n+3}{2} \right) (2n+3)} \left[\ln \left(\frac{k_D \eta_0}{l} \right) - \frac{5}{6} \right] \left(\frac{l}{k_D \eta_0} \right)^3, \quad n > -3/2. \quad (5.25)$$

For $-3 < n < -3/2$, using Eqs. (4.12) and (4.13) and keeping only the highest-order terms in l , we obtain

$$l^2 C_l^{EE(T)} = 2^{2n-5} \frac{49}{625} (2\pi)^{2n+12} \left[G\eta_0^2 z_{\text{eq}} \ln \left(\frac{z_{\text{in}}}{z_{\text{eq}}} \right) \right]^2 \frac{\Gamma(-2n-3)}{\Gamma^2(-n-1)\Gamma^2(\frac{n+3}{2})} \frac{B_0^4(4n^2+3)}{(2n+3)(n+1)(n+3)} \left(\frac{l}{k_D \eta_0} \right)^{2n+6},$$

$$-3 < n < -3/2. \quad (5.26)$$

From the properties of radial functions, Hu and White place upper bounds on how fast various power spectra can grow with l (see Eq. (78) of [53]). In particular, tensor polarization power spectra can grow no faster than $l^2 C_l^{EE, BB(T)} \propto l^2$. Our results for the tensor E- and B-type (Sec. V B 2) polarization power spectra seem to violate this constraint for $n > -2$ by an additional factor of l , which arises from numerical approximations as in the second line of Eq. (4.22). Within the tensor integral solutions of Eqs. (4.21), (5.22), and (5.29), we have to evaluate integrals of the form $\int_0^{x_0} dx [j_2(x)/x][j_l(x_0-x)/(x_0-x)^p]$. The piece $j_2(x)/x$ comes from the gravitational wave solution \dot{h} of Eq. (3.19) whereas the piece $j_l(x_0-x)/(x_0-x)^p$ comes from the radial functions. In Ref. [53], only the radial function properties are used to determine the upper bounds on the power spectra growth rate, whereas the source behavior has been entirely neglected. Our numerical approximation in Eq. (4.22) takes into account the source behavior, i.e. $j_2(x)/x$, and this introduces an additional factor of l in the resulting power spectra. Note that besides the tensor polarization power spectra, all the remaining power spectra conform to the growth constraints given by Ref. [53].

2. B-type Polarization

The B-type polarization integral solution for tensor perturbations is [53]

$$\frac{B_l^{(T)}(\eta_0, k)}{2l+1} = -\sqrt{6} \int_0^{\eta_0} d\eta \dot{\tau} e^{-\tau} P^{(T)} \beta_l^{(T)}[k(\eta_0 - \eta)], \quad (5.27)$$

where

$$\beta_l^{(T)}(x) = \frac{1}{2} \left[j'_l(x) + 2 \frac{j_l(x)}{x} \right] \quad (5.28)$$

is the tensor B-type polarization radial function. Using Eqs. (4.19), (3.19) and (5.5), and defining $x \equiv k\eta$ and $x_0 \equiv k\eta_0$, we approximate the tensor B-type polarization integral solution as

$$\frac{B_l^{(T)}(\eta_0, k)}{2l+1} \simeq \frac{\sqrt{6}}{3} (2\pi) \left[G\eta_0^2 z_{\text{eq}} \ln \left(\frac{z_{\text{in}}}{z_{\text{eq}}} \right) \right] \Pi^{(T)}(k) \int_0^{x_0} dx \frac{j_2(x)}{x} \left[(l+2) \frac{j_l(x_0-x)}{x_0-x} - j_{l+1}(x_0-x) \right]. \quad (5.29)$$

A similar manipulation as in Eq. (4.22) gives

$$\frac{B_l^{(T)}(\eta_0, k)}{2l+1} \simeq \frac{7}{100} (2\pi)^2 \sqrt{l} \left[G\eta_0^2 z_{\text{eq}} \ln \left(\frac{z_{\text{in}}}{z_{\text{eq}}} \right) \right] \frac{\Pi^{(T)}(k)}{k\eta_0} \left[l \frac{J_{l+3}(k\eta_0)}{k\eta_0} - J_{l+4}(k\eta_0) \right]. \quad (5.30)$$

Substituting Eq. (5.30) into (5.2) and using Eq. (2.22), we obtain

$$C_l^{BB(T)} = \frac{49}{10000} (2\pi)^{2n+12} l \left[G\eta_0^2 z_{\text{eq}} \ln \left(\frac{z_{\text{in}}}{z_{\text{eq}}} \right) \right]^2 \frac{B_0^4 \eta_0}{\Gamma^2(\frac{n+3}{2}) (2n+3)(k_D \eta_0)^3}$$

$$\times \int_0^{k_D} dk \left[1 + \frac{n}{n+3} \left(\frac{k}{k_D} \right)^{2n+3} \right] \left[l \frac{J_{l+3}(k\eta_0)}{k\eta_0} - J_{l+4}(k\eta_0) \right]^2. \quad (5.31)$$

For $n > -3/2$, using Eqs. (4.8) and (4.12), we obtain

$$l^2 C_l^{BB(T)} = \frac{49}{5000} (2\pi)^{2n+11} \left[G\eta_0^2 z_{\text{eq}} \ln \left(\frac{z_{\text{in}}}{z_{\text{eq}}} \right) \right]^2 \frac{B_0^4}{\Gamma^2(\frac{n+3}{2}) (2n+3)} \left[\ln \left(\frac{k_D \eta_0}{l} \right) - 1 \right] \left(\frac{l}{k_D \eta_0} \right)^3, \quad n > -3/2.$$

$$(5.32)$$

For $-3 < n < -3/2$, a similar calculation gives

$$l^2 C_l^{BB(T)} = 2^{2n-2} \frac{49}{625} (2\pi)^{2n+12} \left[G\eta_0^2 z_{\text{eq}} \ln \left(\frac{z_{\text{in}}}{z_{\text{eq}}} \right) \right]^2 \frac{\Gamma(-2n-3)}{\Gamma^2(-n-1)\Gamma^2(\frac{n+3}{2})} \frac{-B_0^4 n}{(2n+3)(n+1)(n+3)} \left(\frac{l}{k_D \eta_0} \right)^{2n+6},$$

$$-3 < n < -3/2. \quad (5.33)$$

VI. CROSS-CORRELATION POWER SPECTRA

Since temperature Θ_l has electric parity $(-1)^l$, only E_l couples to Θ_l in the Thomson scattering and hence $C_l^{\Theta E}$ is the only possible cross correlation. The cross-correlation power spectra are defined similarly as the temperature and polarization power spectra:

$$C_l^{\Theta E(X)} = \frac{4}{\pi} \int dk k^2 \frac{\Theta_l^{(X)}(\eta_0, k)}{2l+1} \frac{E_l^{(X)*}(\eta_0, k)}{2l+1}, \quad (6.1)$$

where X stands for V or T .

A. Vector Cross-Correlation Power Spectra

As discussed in Ref. [53] and shown in its Fig. 5, the vector dipole radial function $j_l^{(1V)}$ does not correlate well with its E-type polarization radial function $\epsilon_l^{(V)}$ whereas its quadrupole radial function $j_l^{(2V)}$ does. Therefore to compute the vector cross-correlation power spectra, we need to retain the term proportional to $j_l^{(2V)}$ in the vector temperature integral solution, though in the calculation of the temperature power spectra, we have neglected it since it is suppressed relative to the $j_l^{(1V)}$ term.

Beginning with Eq. (4.5), retaining the $j_l^{(2V)}$ term, neglecting the vector potential, and using Eqs. (4.4) and (5.5), we arrive at the following vector temperature integral solution as in Eq. (4.6):

$$\frac{\Theta_l^{(V)}(\eta_0, k)}{2l+1} \sim \sqrt{\frac{l(l+1)}{2}} \Omega(\eta_{\text{dec}}, k) \left\{ \frac{j_l(k\eta_0)}{k\eta_0} + \frac{1}{3} \frac{k}{\dot{\tau}(\eta_{\text{dec}})} \left[(l-1) \frac{j_l(k\eta_0)}{(k\eta_0)^2} - \frac{j_{l+1}(k\eta_0)}{k\eta_0} \right] \right\}. \quad (6.2)$$

Substituting Eqs. (6.2) and (5.6) into (6.1), using Eqs. (3.12) and (2.18), and neglecting the baryon inertia, we obtain

$$\begin{aligned} C_l^{\Theta E(V)} = & -\frac{(2\pi)^{2n+11}}{3} \sqrt{l(l-1)(l+1)(l+2)} \left(\frac{\eta_{\text{dec}}}{\eta_0} \right)^2 \frac{v_A^4 \eta_0^4}{\Gamma^2(\frac{n+3}{2}) (2n+3)(k_D \eta_0)^3} \\ & \times \int_0^{k_D} dk k^3 \left(\frac{k}{k_*} \right) \left[1 + \frac{n}{n+3} \left(\frac{k}{k_D} \right)^{2n+3} \right] \left\{ (l+1) \frac{J_{l+1/2}^2(k\eta_0)}{(k\eta_0)^3} - \frac{J_{l+1/2}(k\eta_0) J_{l+3/2}(k\eta_0)}{(k\eta_0)^2} \right. \\ & \left. + \frac{1}{3} \left(\frac{k}{k_*} \right) \left[(l^2-1) \frac{J_{l+1/2}^2(k\eta_0)}{(k\eta_0)^4} - 2l \frac{J_{l+1/2}(k\eta_0) J_{l+3/2}(k\eta_0)}{(k\eta_0)^3} + \frac{J_{l+3/2}^2(k\eta_0)}{(k\eta_0)^2} \right] \right\}, \end{aligned} \quad (6.3)$$

where again we have defined $k_* \equiv \dot{\tau}(\eta_{\text{dec}})$. The first two terms within the curly bracket arise from correlating $j_l^{(1V)}$ with $\epsilon_l^{(V)}$. Numerical calculation shows that these two terms always approximately cancel out, thus supporting the claim of Ref. [53] that $j_l^{(1V)}$ does not correlate well with $\epsilon_l^{(V)}$. The remaining three terms arise from correlating $j_l^{(2V)}$ with $\epsilon_l^{(V)}$. In the limit $l \gg 1$, these terms and the three Bessel terms within the vector E-type polarization power spectrum expression of Eq. (5.8) are almost identical. Therefore to simplify the calculation, we will again consider only the term proportional to $J_{l+3/2}^2(k\eta_0)$ and note at the end how good this approximation is. Apart from an overall minus sign here, the resulting power spectra for all cases are approximately equal to the corresponding vector E- and B-type polarization power spectra, given in Eqs. (5.9) and (5.11) to (5.14).

Since we have retained only one of the five terms in the vector cross-correlation power spectrum expression of Eq. (6.3), accuracy here is worse than that of the corresponding E-type polarization power spectra where we have neglected two terms. Our approximation tends to overestimate, due to the reductions arising from the two cross terms in Eq. (6.3). For $n \geq 2$, it is good to within 50%, with accuracy improves as n increases. For $-3 < n < -2$, accuracy is not as good, especially for $l \gtrsim 400$, but always within a factor of a few.

B. Tensor Cross-Correlation Power Spectra

Using Eqs. (4.24), (5.23), and (6.1), we obtain the tensor cross-correlation power spectrum expression

$$C_l^{\Theta E(T)} = \frac{49}{5000} (2\pi)^{2n+12} l^3 \left[G\eta_0^2 z_{\text{eq}} \ln \left(\frac{z_{\text{in}}}{z_{\text{eq}}} \right) \right]^2 \frac{B_0^4 k_D}{\Gamma^2 \left(\frac{n+3}{2} \right) (2n+3)(k_D \eta_0)^4} \\ \times \int_0^{k_D} dk k^{-2} \left[1 + \frac{n}{n+3} \left(\frac{k}{k_D} \right)^{2n+3} \right] \left\{ \left[1 - \frac{l^2}{2(k\eta_0)^2} \right] J_{l+3}^2(k\eta_0) + \frac{J_{l+3}(k\eta_0) J_{l+4}(k\eta_0)}{k\eta_0} \right\}. \quad (6.4)$$

For $n > -3/2$, using Eq. (4.12) and keeping only the highest-order terms in l , we obtain

$$l^2 C_l^{\Theta E(T)} = \frac{49}{3750} (2\pi)^{2n+11} \left[G\eta_0^2 z_{\text{eq}} \ln \left(\frac{z_{\text{in}}}{z_{\text{eq}}} \right) \right]^2 \frac{B_0^4}{\Gamma^2 \left(\frac{n+3}{2} \right) (2n+3)} \left(\frac{l}{k_D \eta_0} \right)^3, \quad n > -3/2. \quad (6.5)$$

For $-3 < n < -3/2$, a similar calculation gives

$$l^2 C_l^{\Theta E(T)} = 2^{2n-4} \frac{49}{625} (2\pi)^{2n+12} \left[G\eta_0^2 z_{\text{eq}} \ln \left(\frac{z_{\text{in}}}{z_{\text{eq}}} \right) \right]^2 \frac{\Gamma(-2n-1)}{\Gamma^2(-n) \Gamma^2 \left(\frac{n+3}{2} \right)} \frac{B_0^4 (2n-1)}{(2n+3)(n+3)} \left(\frac{l}{k_D \eta_0} \right)^{2n+6}, \\ -3 < n < -3/2. \quad (6.6)$$

VII. RESULTS AND DISCUSSION

The CMB power spectra generated by a stochastic magnetic field are plotted for $l = 5$ to $l = 500$ in Figs. 1, 2, and 3. The magnetic field for each plot is normalized to comoving amplitude $B_0 = 10^{-9}$ G; the amplitude of each power spectrum scales as $(B_0/10^{-9}$ G)⁴. The damping scale for each plot is chosen to be $k_D = 4.5$ Mpc⁻¹; this is the scale at which one e-folding of Alfvén damping via photon viscosity has occurred by equality [52], i.e. $\int_0^{\eta_{\text{eq}}} d\eta D/2 = 1$, where $D(\eta) = 0.2(1+z)k^2 l_\gamma(\eta)$ is a time-dependent damping coefficient and l_γ is the photon physical mean-free path [37]. For $n > -3$ the fluctuations at small scales are dominant, and the cutoff scale will determine the overall amplitude of the fluctuations. These plots do *not* include the effect of magnetic field damping: the amplitude of the magnetic field will be suppressed like $\exp(-k^2/k_D^2)$ for small scales with $k > k_D$. Thus for $l > l_D$ the displayed power spectrum must be reduced by approximately $\exp(-l^2/l_D^2)$, where $l_D \simeq k_D \eta_0$. With a magnetic damping length of $L_D = 2\pi/k_D = 1.4$ Mpc, the magnetic field damping has negligible effect on the microwave background fluctuations for $l < 500$. For the tensor perturbations, we assume $z_{\text{in}}/z_{\text{eq}} = 10^9$ as in Ref. [52]; the resulting fluctuations, however, depend only logarithmically on z_{in} .

Figure 1 shows the separate vector and tensor contributions to the CMB power spectra for two different values of n . For the vector perturbations, the EE, BB, and ΘE power spectra are all essentially identical. Naively, the ΘE cross-correlation would be expected to be larger than the polarization power spectra simply because the temperature fluctuations are larger than the polarization fluctuations. However, the temperature fluctuations are dominated by the vector dipole term, which correlates poorly with the radial function describing E-type polarization. Thus the ΘE spectrum is dominated by a subdominant temperature contribution arising from the vector quadrupole term, which then coincidentally renders the spectrum a form similar to the E-type polarization itself. In our calculations, we assume all the vector anisotropies are due to the vorticity at decoupling, as illustrated by Eqs. (3.14), (4.6), (5.6), and (5.17). This assumption is reasonable because after decoupling, magnetic fields do not couple to the baryons and hence the vorticity becomes negligible. Note that while $n \rightarrow -3$ corresponds to a scale-invariant magnetic field, the vector power spectrum is not flat for this value. The reason is that the vorticity, Eq. (3.12), has an extra factor of k compared to the magnetic field itself. The vector cross-correlation is always negative; its absolute value is plotted.

For the tensor perturbations, the polarization power spectra are actually comparable to the temperature power spectrum for $n > 0$. This is because both the temperature and polarization fluctuations are due to the intrinsic temperature quadrupole moments, which arise from the gravitational wave solution \dot{h} of Eq. (3.19) instead of being generated via free streaming the dipoles as in the case of the vector perturbations. For $n > -3/2$, the gravitational wave source is approximately independent of k and the resulting power spectra possess the well-known behavior of a white noise source $l^2 C_l \propto l^3$. As expected, the tensor power spectrum is flat for $n \rightarrow -3$ since we have a scale-invariant magnetic field for this value. The tensor cross-correlation is always positive.

The difference between the sign of the vector and tensor cross-correlations can be understood from the geometric properties of the projection of their corresponding temperature and polarization sources as anisotropies on the sky [53]. The sign of the vector and tensor cross-correlations is determined by respectively (cf. Eq. (80) of Ref. [53])

$$\text{sgn}[C_l^{\Theta E(V)}] = -\text{sgn}[P^{(V)}(\dot{\tau} P^{(V)})], \quad (7.1)$$

$$\text{sgn}[C_l^{\Theta E(T)}] = \text{sgn}[P^{(T)}(\dot{\tau} P^{(T)} - \dot{h})]. \quad (7.2)$$

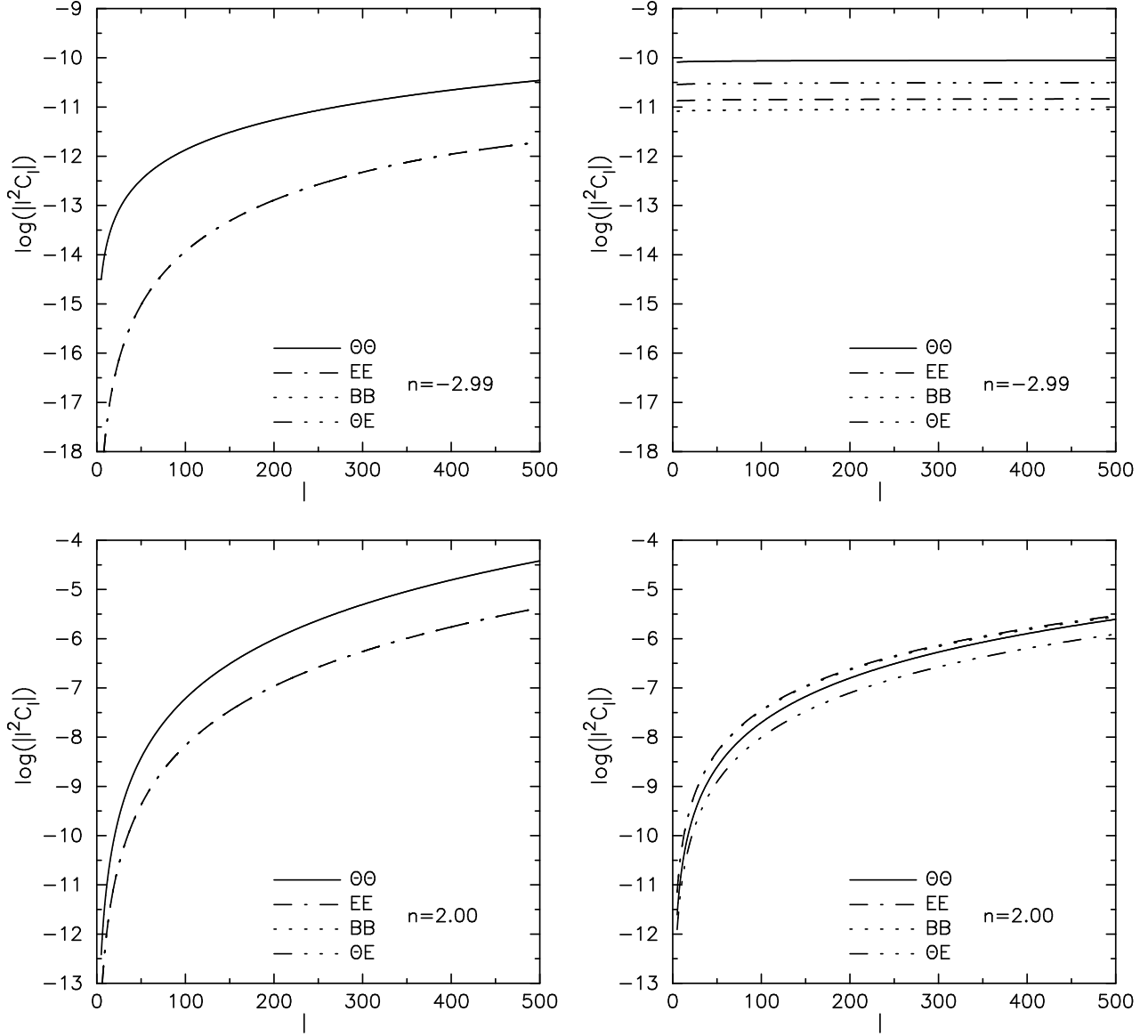


FIG. 1. The microwave background power spectra for vector (left panels) and tensor (right panels) perturbations from a power-law stochastic magnetic field with power-law index n . The vertical axis scales with magnetic field amplitude as $(B_0/10^{-9} \text{ G})^4$. The magnetic damping scale is chosen to be $k_D = 4.5 \text{ Mpc}^{-1}$. For the tensor perturbations, we assume $z_{\text{in}}/z_{\text{eq}} = 10^9$.

The sign of the vector cross-correlation is therefore always opposite to that of the tensor cross-correlation.

Each panel in Fig. 2 shows the total vector plus tensor contribution for the various power spectra for a particular value of n . For $n \geq 0$ the ΘE cross-correlation has a zero which appears as a cusp since the absolute value is plotted. Each panel in Fig. 3 replots one of the four power spectra for a range of spectral indices n . As the spectral index becomes greater than zero, the amplitudes become quite large. For a scale-invariant $n \rightarrow -3$ spectral index and a comoving $B_0 = 10^{-9}$ G, the temperature and polarization power spectra are roughly the same amplitude as expected from scale-invariant density perturbations normalized to COBE (i.e., CMB fluctuations in “standard” cosmological models). But for $n = 0$, the power spectra are all essentially a factor of 1000 larger at $l = 500$. Observational limits will be much stronger for causal fields than for scale-invariant fields.

To estimate the potential observational limits on stochastic magnetic fields, the induced microwave background anisotropies must be large enough to be disentangled from the anisotropies arising from density perturbations. Current temperature maps give power spectrum measurements with error bars on the order of 10% out to $l = 400$ for bins of width $\Delta l = 50$ [9,11]. The MAP satellite, set for an imminent launch, will make temperature measurements out to around $l = 800$ and will reach the cosmic variance limit, $\Delta C_l = (2l + 1)^{-1/2} C_l$, out to $l = 400$ [72]. By the end of the decade, and perhaps within five years, we can expect a cosmic-variance limited temperature power spectrum measurement to $l = 3000$. Polarization fluctuations will also be detected soon, and the progress in their measurement will likely lag temperature fluctuations by about a decade. A rough but conservative estimate is that a magnetic-field signal which is at least 10% of the dominant density-perturbation signal will be detectable. The ultimate sensitivity in measuring the temperature power spectrum at, say, $l = 500$ will be significantly better than this, and the extent to which magnetic fields can be constrained depends more on the degeneracy of the magnetic field signal with shifts in various cosmological parameters. Basic statistical techniques for pursuing such an analysis are well-known (see, e.g., [56]) and will be considered elsewhere.

Using this crude 10% criterion, we can constrain stochastic magnetic fields from current temperature measurements by simply comparing the predicted amplitude at $l = 500$ to the amplitude of current measurements, which is on the order of $l^2 C_l \simeq 10^{-10}$. We assume that the remainder of the power spectrum is used for discrimination between the signals from magnetic fields and other temperature power spectrum contributors. For the scale-invariant magnetic field with $n \rightarrow -3$, a field amplitude of $B_0 = 10^{-9}$ G gives anisotropies at the same level as current measurements, so the limit from temperature perturbations will be around 6×10^{-10} G. As n increases towards causal values, the amplitude of the small-scale temperature fluctuations increases, so the limits become stronger. At $n = 0$, $l^2 C_l$ at $l = 500$ is about 10^3 larger than for $n = -2.99$, which gives a limit on B_0 smaller by a factor of $10^{3/4} = 5.6$, or 10^{-10} G. For the causal $n = 2$, the limit on B_0 is as small as 3×10^{-11} G. These are the strongest current limits on large-scale stochastic magnetic fields. The addition of E-type polarization measurements will only modestly improve these limits, since the ratio of the E-type polarization to temperature power spectra is roughly the same for stochastic magnetic fields and the dominant density perturbations.

Ultimately, B-type polarization has the greatest potential for constraining primordial magnetic fields. This is a cleaner signature, because primordial scalar (density) perturbations produce none [54,69]. Aside from polarized foreground emission, the only other expected sources are from primordial tensor perturbations and from gravitational lensing [57]. Tensor perturbations with a spectrum near scale-invariant will give significant anisotropies only at large angular scales ($l < 100$), while lensing contributes mainly at small angular scales ($l > 500$). Stochastic magnetic fields will contribute on intermediate scales and should be clearly distinguishable. If foreground emission can be separated from its frequency dependence, limits on B_0 from B-type polarization should be determined purely by measurement error bars on C_l^{BB} . With sufficiently sensitive receivers, limits of 10^{-11} G for $n = 2$ are possible. Note that a primordial magnetic field also generates an additional B-type polarization signal via Faraday rotation of the CMB polarization [41]. This signal will be negligible compared to the direct B-polarization signal for any frequency of practical interest.

Proper interpretation of these results requires a clear understanding of the field amplitude B_0 we employ. Recall that we consider a stochastic magnetic field with a power-law power spectrum down to some physical damping scale k_D ; the magnetic field will be exponentially suppressed on scales smaller than the damping scale. The physical damping of MHD modes is due to photon and neutrino viscosities [36,37]; the mechanism itself is somewhat similar to the Silk damping of density perturbations [73], and a crude estimate of the damping scale is $k_D = 4.5 \text{ Mpc}^{-1}$. Given a power law and damping scale, a complete specification of the magnetic field requires only a normalization. To specify the normalization, we define B_0 as the rms magnetic field strength of this field. This normalization does not require any smoothing scale other than the physical damping scale. We belabor this point because in some of the cosmological magnetic field literature, the field is normalized as the average value of the field convolved with a Gaussian window function of length λ [35,48,49,52]. With this scheme, it makes no sense to ask for a single normalization of the magnetic field, but rather only the normalization B_λ on a given length scale λ ; then $B_\lambda^2 \propto \lambda^{-(n+3)}$. As an example, the vector temperature power spectrum for $n > -3/2$ will now be given by [c.f. Eq. (4.9)]

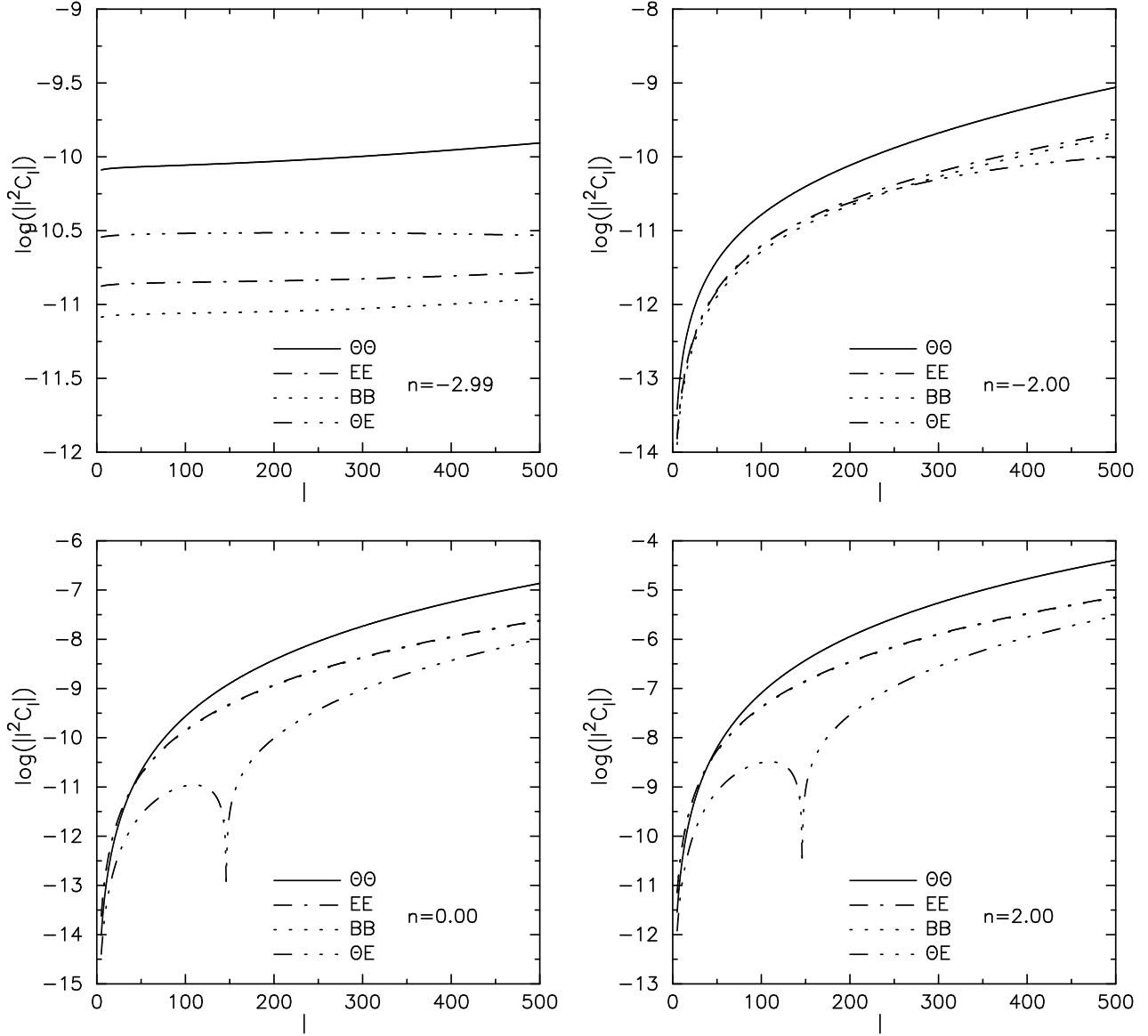


FIG. 2. The microwave background power spectra for vector plus tensor perturbations from a power-law stochastic magnetic field with power-law index n . Each panel shows the various power spectra at fixed n . The vertical axis scales with magnetic field amplitude as $(B_0/10^{-9} \text{ G})^4$. The magnetic damping scale is chosen to be $k_D = 4.5 \text{ Mpc}^{-1}$. For the tensor perturbations, we assume $z_{\text{in}}/z_{\text{eq}} = 10^9$.

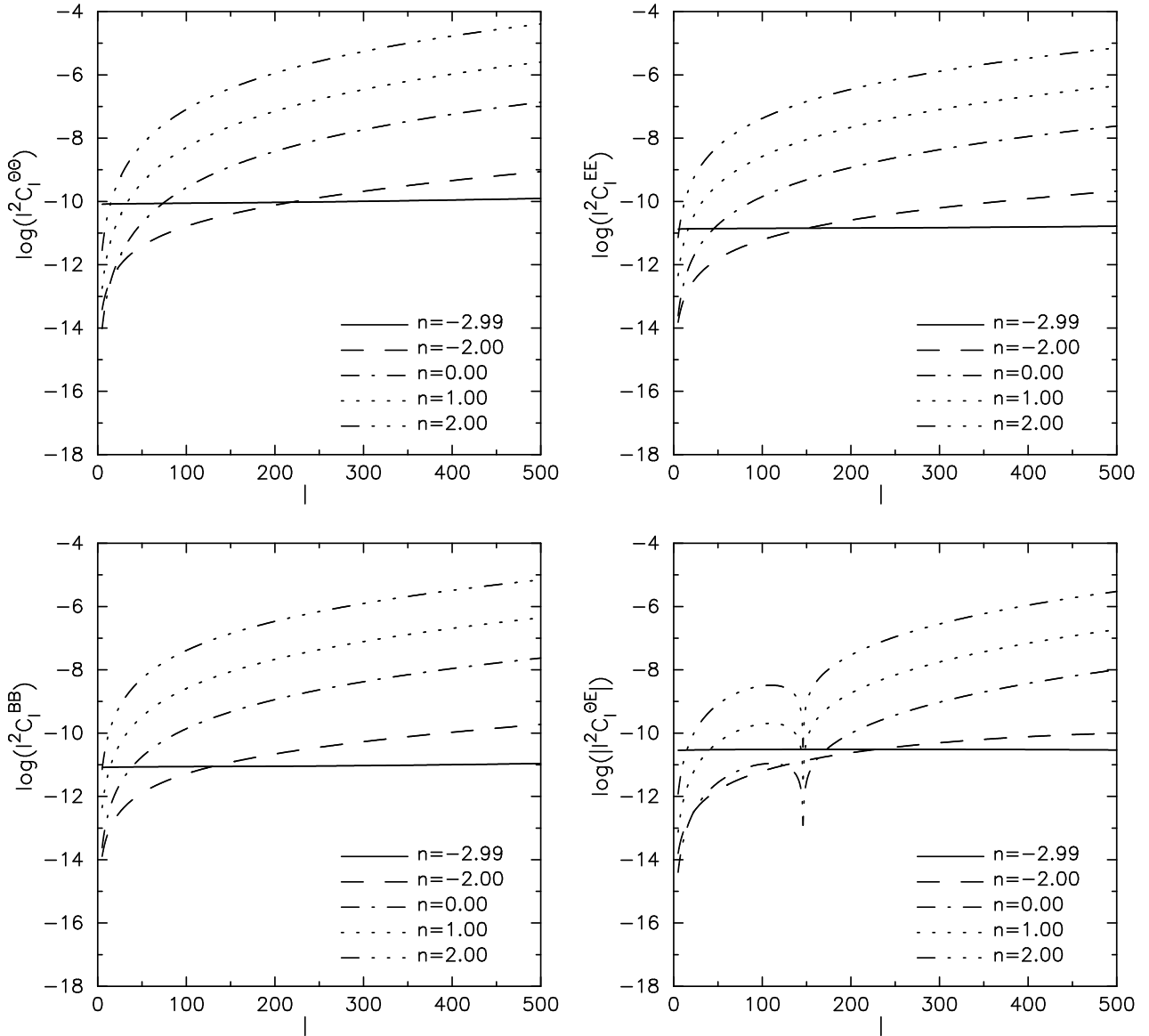


FIG. 3. Same as in Fig. 2, except that each panel shows a single power spectrum for various values of n .

$$l^2 C_l^{\Theta\Theta(V)} = 2(2\pi)^4 \left(\frac{\eta_{\text{dec}}}{\eta_0} \right)^2 \left(\frac{\lambda}{\eta_0} \right)^{2n+6} \frac{(k_D \eta_0)^{2n+4} v_{A\lambda}^4 l^4}{\Gamma^2 \left(\frac{n+3}{2} \right) (2n+3)}, \quad n > -3/2, \quad (7.3)$$

where $v_{A\lambda} = B_\lambda / [4\pi(\rho_{\gamma 0} + p_{\gamma 0})]^{1/2}$. The two normalization methods are equivalent if λ is always taken to be the physical magnetic damping scale $\lambda_D = 2\pi/k_D$.

All of the results in this paper have been obtained via analytic approximations to the exact solutions. For the vector temperature and B-type polarization and tensor power spectra, the accuracy of the results is as good as the quality of the analytic approximations to various expressions, except that the vector temperature case has neglected an additional 10% temperature contribution coming from the angular dependence of polarization. These approximations are all discussed in the text; in sum, they are good to at least 20% for $n \geq -5/2$ and within 50% for $-3 < n < -5/2$ over the range of parameters considered. Meanwhile, accuracy of the analytic approximations for the vector E-type polarization and cross-correlation power spectra is not as good since we have only considered the dominant term in Eqs. (5.8) and (6.3) respectively. For $n \geq -2$, the error is no larger than 50%, whereas for $-3 < n < -2$, the accuracy is only good to within a factor of a few since the neglected terms in Eqs. (5.8) and (6.3) are becoming important in this regime. It is important to point out that errors of these analytic approximations will have negligible effects on the estimation of the magnetic field limits, since the amplitude of each power spectrum scales as B_0^4 . Note that for the vector perturbations, our analytic approximations tend to underestimate for B-type polarization and overestimate for E-type polarization and cross-correlation; thus in reality we should have $l^2 C_l^{BB(V)} \gtrsim l^2 C_l^{EE(V)} \gtrsim |l^2 C_l^{\Theta E(V)}|$. In fact, it has been pointed out in Ref. [53] that the vector CMB polarization is dominated by the B-type modes. Our analytic treatment here, however, is insufficient to render a more quantitative statement regarding the relative strength of the vector E-type and B-type polarization for magnetic field sources.

This paper has only considered vector and tensor metric perturbations. Stochastic magnetic fields will also produce scalar perturbations. This case is significantly more complex due to physical compensation effects and the large number of terms involved in the relevant expressions. We have performed analytic computations for the scalar case as well. While the Sachs-Wolfe effect arising from the scalar perturbations will always be negligible to the vector and tensor terms, the Doppler term can be significant. For vorticity perturbations, the velocity vector tends to be perpendicular to the Fourier mode vector, so that the Doppler contribution is suppressed; but for scalar perturbations, the velocity vector is aligned with the Fourier mode vector, and the resulting temperature fluctuation is much larger. The total CMB fluctuations from magnetic field scalar perturbations can be somewhat larger than those from vector or tensor perturbations due to this effect, so the upper limits on magnetic field strengths will be a bit more stringent than those obtained here. These scalar results will be presented in a forthcoming companion paper [58].

ACKNOWLEDGMENTS

We thank R. Durrer, W. Hu, K. Jedamzik, and M. White for discussions. This work has been supported by the COBASE program of the U.S. National Research Council and by the NASA Astrophysics Theory Program through grant NAG5-7015. A.K. is a Cotrell Scholar of the Research Corporation. T.K. acknowledges the kind hospitality of Rutgers University.

APPENDIX A: DERIVATION OF THE VECTOR ISOTROPIC SPECTRUM

Our objective is to derive the vector isotropic spectrum $|\Pi^{(V)}(k)|^2$ defined in Eq. (2.17), which will be useful for calculating vector CMB power spectra. Using Eq. (2.14), the two-point correlation function of $\Pi_i^{(V)}$ is given by

$$\langle \Pi_i^{(V)}(\mathbf{k}) \Pi_i^{(V)*}(\mathbf{k}') \rangle = P_{ib} \hat{k}_a P'_{id} \hat{k}'_c \langle \tau_{ab}^{(B)}(\mathbf{k}) \tau_{cd}^{(B)*}(\mathbf{k}') \rangle, \quad (A1)$$

where $P'_{id} = \delta_{id} - \hat{k}'_i \hat{k}'_d$. We simplify our calculation by splitting the electromagnetic stress-energy tensor into two pieces: $\tau_{ij}^{(B)}(\mathbf{k}) = \tau_{ij}^{(B,1)}(\mathbf{k}) + \tau_{ij}^{(B,2)}(\mathbf{k})$ where

$$\tau_{ij}^{(B,1)}(\mathbf{k}) \equiv \frac{1}{(2\pi)^3} \frac{1}{4\pi} \int d^3 p B_i(\mathbf{p}) B_j(\mathbf{k} - \mathbf{p}), \quad (A2a)$$

$$\tau_{ij}^{(B,2)}(\mathbf{k}) \equiv -\frac{1}{(2\pi)^3} \frac{1}{8\pi} \delta_{ij} \int d^3 p B_l(\mathbf{p}) B_l(\mathbf{k} - \mathbf{p}). \quad (A2b)$$

The two-point correlation function of the electromagnetic stress-energy tensor in Eq. (A1) will now be described by a sum of four two-point correlation functions:

$$\begin{aligned}\langle \tau_{ab}^{(B)}(\mathbf{k}) \tau_{cd}^{(B)*}(\mathbf{k}') \rangle &= \langle \tau_{ab}^{(B,1)}(\mathbf{k}) \tau_{cd}^{(B,1)*}(\mathbf{k}') \rangle + \langle \tau_{ab}^{(B,1)}(\mathbf{k}) \tau_{cd}^{(B,2)*}(\mathbf{k}') \rangle \\ &\quad + \langle \tau_{ab}^{(B,2)}(\mathbf{k}) \tau_{cd}^{(B,1)*}(\mathbf{k}') \rangle + \langle \tau_{ab}^{(B,2)}(\mathbf{k}) \tau_{cd}^{(B,2)*}(\mathbf{k}') \rangle.\end{aligned}\quad (\text{A3})$$

Only $\langle \tau_{ab}^{(B,1)} \tau_{cd}^{(B,1)*} \rangle$ above has a non-vanishing contribution toward the two-point correlation function of $\Pi_i^{(V)}$ in Eq. (A1), since each of the remaining correlation functions in Eq. (A3) contains either δ_{ab} , δ_{cd} , or both, and will vanish when they are acted upon by $P_{ib} \hat{k}_a P'_{id} \hat{k}'_c$. We can now rewrite Eq. (A1) as

$$\langle \Pi_i^{(V)}(\mathbf{k}) \Pi_i^{(V)*}(\mathbf{k}') \rangle = P_{ib} \hat{k}_a P'_{id} \hat{k}'_c \langle \tau_{ab}^{(B,1)}(\mathbf{k}) \tau_{cd}^{(B,1)*}(\mathbf{k}') \rangle. \quad (\text{A4})$$

We can evaluate the two-point correlation function $\langle \tau_{ab}^{(B,1)} \tau_{cd}^{(B,1)*} \rangle$ as follows. Beginning with the definition of Eq. (A2a), we apply Wick's theorem

$$\begin{aligned}\langle B_i(\mathbf{k}_i) B_j(\mathbf{k}_j) B_l(\mathbf{k}_l) B_m(\mathbf{k}_m) \rangle &= \langle B_i(\mathbf{k}_i) B_j(\mathbf{k}_j) \rangle \langle B_l(\mathbf{k}_l) B_m(\mathbf{k}_m) \rangle + \langle B_i(\mathbf{k}_i) B_l(\mathbf{k}_l) \rangle \langle B_j(\mathbf{k}_j) B_m(\mathbf{k}_m) \rangle \\ &\quad + \langle B_i(\mathbf{k}_i) B_m(\mathbf{k}_m) \rangle \langle B_j(\mathbf{k}_j) B_l(\mathbf{k}_l) \rangle\end{aligned}\quad (\text{A5})$$

and the reality condition $B_i^*(\mathbf{k}) = B_i(-\mathbf{k})$, and finally use Eq. (2.1) for the form of the stochastic magnetic field two-point correlation function to arrive at (see also [52])

$$\begin{aligned}\langle \tau_{ab}^{(B,1)}(\mathbf{k}) \tau_{cd}^{(B,1)*}(\mathbf{k}') \rangle &= \frac{1}{(4\pi)^2} \int d^3 p P(p) P(|\mathbf{k} - \mathbf{p}|) [(\delta_{ac} - \hat{p}_a \hat{p}_c)(\delta_{bd} - (\widehat{\mathbf{k} - \mathbf{p}})_b (\widehat{\mathbf{k} - \mathbf{p}})_d) \\ &\quad + (\delta_{ad} - \hat{p}_a \hat{p}_d)(\delta_{bc} - (\widehat{\mathbf{k} - \mathbf{p}})_b (\widehat{\mathbf{k} - \mathbf{p}})_c)] \delta(\mathbf{k} - \mathbf{k}').\end{aligned}\quad (\text{A6})$$

Substitute Eq. (A6) into Eq. (A4) and define $\gamma \equiv \hat{\mathbf{k}} \cdot \hat{\mathbf{p}}$, $\beta \equiv \hat{\mathbf{k}} \cdot (\widehat{\mathbf{k} - \mathbf{p}})$, and $\mu \equiv \hat{\mathbf{p}} \cdot (\widehat{\mathbf{k} - \mathbf{p}})$ to obtain the two-point correlation function of the vector $\Pi_i^{(V)}$:

$$\langle \Pi_i^{(V)}(\mathbf{k}) \Pi_i^{(V)*}(\mathbf{k}') \rangle = \frac{1}{(4\pi)^2} \int d^3 p P(p) P(|\mathbf{k} - \mathbf{p}|) [(1 - \gamma^2)(1 + \beta^2) + \gamma\beta(\mu - \gamma\beta)] \delta(\mathbf{k} - \mathbf{k}'). \quad (\text{A7})$$

The integral above is similar to the mode-coupling integral $I^2(k)$ in Eq. (11) of Ref. [50]. Although it cannot be evaluated analytically, terms within the square bracket are products of cosine factors; hence the square bracket itself can be approximated by unity, which has essentially been done in Ref. [52]. Comparing with Eq. (2.17) gives

$$|\Pi^{(V)}(k)|^2 \simeq \frac{1}{(2\pi)^2} \frac{1}{8} \int d^3 p P(p) P(|\mathbf{k} - \mathbf{p}|). \quad (\text{A8})$$

Using the expression for $P(k)$ in Sec. II and choosing $\hat{\mathbf{k}}$ to be the polar axis, the vector isotropic spectrum becomes

$$|\Pi^{(V)}(k)|^2 \simeq \frac{(2\pi)^{2n+9}}{8} \frac{B_0^4}{\Gamma^2 \left(\frac{n+3}{2}\right) k_D^{2n+6}} \int_0^{k_D} dp p^{n+2} \int_{-1}^1 d\gamma (k^2 + p^2 - 2\gamma kp)^{n/2}. \quad (\text{A9})$$

The integral over γ is

$$\int_{-1}^1 d\gamma (k^2 + p^2 - 2\gamma kp)^{n/2} = \frac{1}{kp(n+2)} [(k+p)^{n+2} - |k-p|^{n+2}], \quad (\text{A10})$$

and the expression within the square bracket above can be approximated as

$$(k+p)^{n+2} - |k-p|^{n+2} \simeq \begin{cases} 2(n+2)k^{n+1}p, & p < k; \\ 2(n+2)kp^{n+1}, & \text{otherwise.} \end{cases} \quad (\text{A11})$$

Substituting Eqs. (A10) and (A11) into Eq. (A9) and evaluating, we finally arrive at the expression for the vector isotropic spectrum, Eq. (2.18).

[1] P.P. Kronberg, *Rep. Prog. Phys.* **57**, 325 (1994).

[2] K.T. Kim, P.P. Kronberg, and P.C. Tribble, *Astrophys. J.* **379**, 80 (1991).

[3] Ya.B. Zeldovich, A.A. Ruzmaikin, and D.D. Sokoloff, *Magnetic Fields in Astrophysics* (Gordon and Breach, New York, 1983).

[4] E.N. Parker, *Cosmical Magnetic Fields* (Oxford University Press, Oxford, 1979).

[5] A. Davis, M. Lilley, and O. Törnqvist, *Phys. Rev. D* **60**, 021301 (1999).

[6] B.P. Schmidt et al., *Astrophys. J.* **507**, 46 (1998).

[7] S. Perlmutter et al., *Astrophys. J.* **517**, 565 (1999).

[8] A.D. Miller et al., *Astrophys. J. Lett.* **524**, L1 (1999).

[9] S. Hanany et al., *Astrophys. J. Lett.* **545**, L5 (2000).

[10] A. Balbi et al., *Astrophys. J. Lett.* **545**, L1 (2000).

[11] P. de Bernardis et al., *Nature*, **404**, 955 (2000).

[12] A.E. Lange et al., *Phys. Rev. D* **63**, 042001 (2001).

[13] C.M. Ko and E.N. Parker, *Astrophys. J.* **341**, 828 (1989).

[14] S.I. Vainshtein and R. Rosner, *Astrophys. J.* **376**, 199 (1991).

[15] R.M. Kulsrud and S.W. Anderson, *Astrophys. J.* **396**, 606 (1992).

[16] F. Cattaneo, *Astrophys. J.* **434**, 200 (1994).

[17] A.V. Gruzinov and P.H. Diamond, *Phys. Rev. Lett.* **72**, 1651 (1994).

[18] E. Blackman, *Phys. Rev. Lett.* **77**, 2694 (1996).

[19] R. Kulsrud, S.C. Cowley, A.V. Gruzinov, and R.N. Sudan, *Phys. Rep.* **283**, 213 (1997).

[20] K. Subramanian, *Phys. Rev. Lett.* **83**, 2957 (1999).

[21] M.S. Turner and L.M. Widrow, *Phys. Rev. D* **37**, 2743 (1988).

[22] S.M. Carroll and G.B. Field, *Phys. Rev. D* **43**, 3789 (1991).

[23] W.D. Garretson, G.B. Field, and S.M. Carroll, *Phys. Rev. D* **46**, 5346 (1992).

[24] B. Ratra, *Astrophys. J. Lett.* **391**, L1 (1992).

[25] M. Gasperini, M. Giovannini, and G. Veneziano, *Phys. Rev. Lett.* **75**, 3796 (1995).

[26] M. Gasperini, M. Giovannini, and G. Veneziano, *Phys. Rev. D* **52**, 6651 (1995).

[27] T. Vachaspati, *Phys. Lett. B* **265**, 258 (1991).

[28] K. Enqvist and P. Olesen, *Phys. Lett. B* **319**, 178 (1993).

[29] J. Quashnock, A. Loeb, and D.N. Spergel, *Astrophys. J. Lett.* **344**, L49 (1989).

[30] B. Cheng and A. Olinto, *Phys. Rev. D* **50**, 2421 (1994).

[31] A.D. Dolgov and J. Silk, *Phys. Rev. D* **47**, 3144 (1993).

[32] K. Enqvist and P. Olesen, *Phys. Lett. B* **329**, 195 (1994).

[33] D. Grasso and H.R. Rubinstein, *Phys. Rep.* in press (2001).

[34] I. Wasserman, *Astrophys. J.* **224**, 337 (1978).

[35] E.-J. Kim, A.V. Olinto, and R. Rosner, *Astrophys. J.* **468**, 28 (1996).

[36] K. Jedamzik, V. Katalinić, and A.V. Olinto, *Phys. Rev. D* **57**, 3264 (1998).

[37] K. Subramanian and J.D. Barrow, *Phys. Rev. D* **58**, 083502 (1998).

[38] J.D. Barrow, P.G. Ferreira, and J. Silk, *Phys. Rev. Lett.* **78**, 3610 (1997).

[39] J. Adams, U.H. Danielsson, D. Grasso, and H. Rubinstein, *Phys. Lett. B* **388**, 253 (1996).

[40] R. Durrer, T. Kahniashvili, and A. Yates, *Phys. Rev. D* **58**, 123004 (1998).

[41] A. Kosowsky and A. Loeb, *Astrophys. J.* **469**, 1 (1996).

[42] E.S. Scannapieco and P.G. Ferreira, *Phys. Rev. D* **56**, 7493 (1997).

[43] D.D. Harari, J.D. Hayward, and M. Zaldarriaga, *Phys. Rev. D* **55**, 1841 (1997).

[44] J.W. Dreher, C.L. Carilli, and R.A. Perley, *Astrophys. J.* **316**, 611 (1987).

[45] R.A. Perley and G.B. Taylor, *Astron. J.* **101**, 1623 (1991).

[46] G.B. Taylor and R.A. Perley, *Astrophys. J.* **416**, 554 (1993).

[47] J.P. Ge and F.N. Owen, *Astron. J.* **105**, 778 (1993).

[48] S. Koh and C.H. Lee, *astro-ph/0006357*, 2000 (unpublished).

[49] D. Lemoine, *Cosmic Microwave Background Anisotropies Generated by a Primordial Magnetic Field*, 1995 Ph.D. Thesis (unpublished).

[50] K. Subramanian and J.D. Barrow, *Phys. Rev. Lett.* **81**, 3575 (1998).

[51] T.R. Seshadri and K. Subramanian, *astro-ph/0012056*, 2000 (unpublished).

[52] R. Durrer, P.G. Ferreira, and T. Kahniashvili, *Phys. Rev. D* **61**, 043001 (2000).

[53] W. Hu and M. White, *Phys. Rev. D* **56**, 596 (1997).

[54] M. Kamionkowski, A. Kosowsky, and A. Stebbins, *Phys. Rev. Lett.* **78**, 2058 (1997).

[55] U. Seljak and M. Zaldarriaga, *Phys. Rev. Lett.* **78**, 2054 (1997).

[56] M. Kamionkowski and A. Kosowsky, *Phys. Rev. D* **57**, 685 (1998).

[57] M. Zaldarriaga and U. Seljak, *Phys. Rev. D* **58**, 023003 (1998).

[58] T. Kahniashvili, A. Mack, and A. Kosowsky, 2001 (in preparation).

- [59] J. Ahonen and K. Enqvist, Phys. Lett. B **382**, 40 (1996).
- [60] J.A. Peacock, *Cosmological Physics* (Cambridge University, Cambridge, 1999).
- [61] L.F. Abbott and R.K. Schaefer, Astrophys. J. **308**, 546 (1986).
- [62] P. Coles and F. Lucchin, *Cosmology: The Origin and Evolution of Cosmic Structure* (Wiley, Chichester, 1995).
- [63] J.D. Jackson, *Classical Electrodynamics* (Wiley, New York, 1975).
- [64] V.F. Mukhanov, H.A. Feldman, and R.H. Brandenberger, Phys. Rep. **215**, 203 (1992).
- [65] J.M. Bardeen, Phys. Rev. D **22**, 1882 (1980).
- [66] R. Durrer, Fundam. Cosm. Phys. **15**, 209 (1994).
- [67] M. Abramowitz and I. Stegun, *Handbook of Mathematical Functions* (Dover, New York, 1972).
- [68] I.S. Gradshteyn and I.M. Ryzhik, *Table of Integrals, Series, and Products*, edited by A. Jeffrey (Academic, San Diego, 1994).
- [69] M. Zaldarriaga and U. Seljak, Phys. Rev. D **55**, 1830 (1997).
- [70] M. Kamionkowski, A. Kosowsky, and A. Stebbins, Phys. Rev. D **55**, 7368 (1997).
- [71] W. Hu and N. Sugiyama, Astrophys. J. **444**, 489 (1995).
- [72] See the MAP home page, URL <http://map.gsfc.nasa.gov>.
- [73] J. Silk, Astrophys. J. **151**, 459 (1968).